

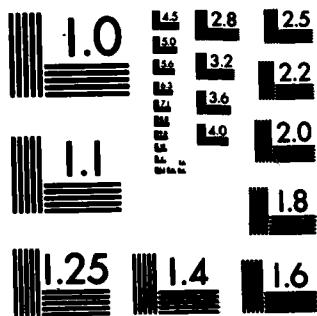
AD-A124 892

CORRELATING RADIO EMISSIONS WITH VISIBLE EMISSIONS FROM 1/1
INDIVIDUAL SOLAR ACTIVE REGIONS(U) AIR FORCE INST OF
TECH WRIGHT-PATERSON AFB OH SCHOOL OF ENGI... C A PUZ
DEC 82 AFIT/GSD/MA/82D-2 F/G 12/1. NL

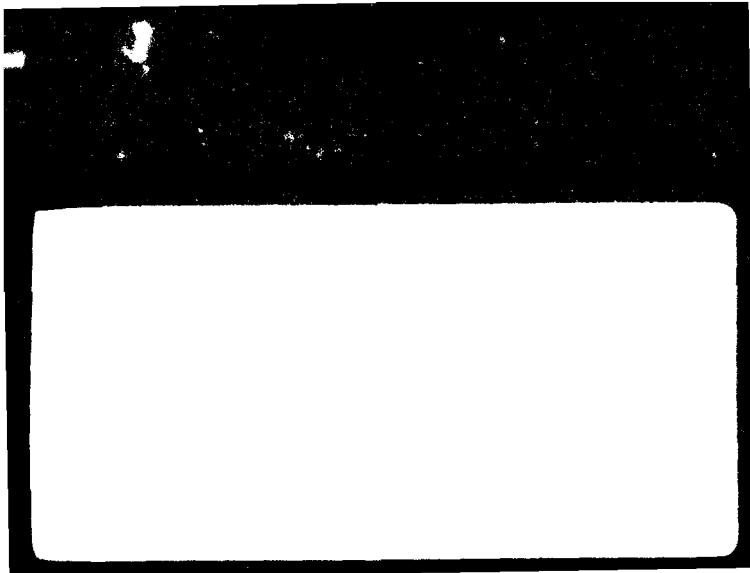
UNCLASSIFIED



END
DATE
INDEXED
83
DTIC



MICROCOPY RESOLUTION TEST CHART
NATIONAL BUREAU OF STANDARDS-1963-A



AFIT/GSO/MA/82D-2

CORRELATING RADIO EMISSIONS WITH
VISIBLE EMISSIONS
FROM INDIVIDUAL SOLAR ACTIVE REGIONS

THESIS

AFIT/GSO/MA/82D-2

Craig A. Puz
Capt USAF

Approved for public release; distribution unlimited

AFIT/GSO/MA/82D-2

CORRELATING RADIO EMISSIONS WITH VISIBLE EMISSIONS
FROM INDIVIDUAL SOLAR ACTIVE REGIONS

THESIS

Presented to the Faculty of the School of Engineering
of the Air Force Institute of Technology

Air University

in Partial Fulfillment of the
Requirements for the Degree of
Master of Science

by

Craig A. Puz, B.S., MBA

Capt USAF

Graduate Space Operations

December 1982



Distribution For	
DTIC	<input checked="" type="checkbox"/>
GR&I	<input type="checkbox"/>
TAB	<input type="checkbox"/>
Announced	<input type="checkbox"/>
Classification	
Distribution/	
Availability Codes	
Dist	Avail and/or
A	Special

Approved for public release; distribution unlimited.

ACKNOWLEDGEMENTS

Many people were indispensable in allowing me to complete this study. I am indebted to Mr. Aunri Gagnon of the Algonquin Radio Observatory, Ottawa, Canada, for the 10.7 cm solar scans and Ms. Helen Coffey, Major Bruce D. Springer, and especially Mr. Ronald W. Buhmann at the National Oceanic and Atmospheric Administration World Data Center, Boulder, Colorado, for the SOON data. Guidance and explanations of the systems for collecting these data were graciously provided by Dr. Morley Bell at Algonquin and Mr. Arnold Star at the Holloman AFB, New Mexico, SOON site. I must also thank all of the members of the first Graduate Space Operations class at the Air Force Institute of Technology for their invaluable support, in particular, Captain John D. Rask and Captain Robert I. Boren. Additionally, I must acknowledge the tireless efforts of Major James J. Lange for helping me to understand the physical phenomena involved in the project and Captain Brian W. Woodruff, my advisor, who always kept me moving in the right direction. Finally, I want to thank my friend, Captain Brian E. Dieffenbach, who helped me keep my perspective throughout the project.

Craig A. Pus

Contents

	<u>Page</u>
Acknowledgement	ii
List of Figures	v
List of Tables	vi
Abstract	vii
I. Introduction	1
Background	1
Statement of the Problem	4
Objective of the Research	4
Methodology	4
Limitations	5
II. Historical Survey	8
SOON Data	8
The 10.7 CM Solar Radio Flux	11
10.7 CM Solar Radio Flux Uses	13
Usefulness	13
Predicted Values	13
10.7 CM Solar Radio Flux Predictive Models.	15
Cautions	16
Long Term Techniques	17
Medium Term Techniques	19
Short Term Techniques	19
III. Methodology	21
Data Reduction	21
Data Comparison	23
Data Analysis	27
Model Development	28
Confidence Interval	33
Other Relationships	35
IV. Conclusions and Recommendations	37
Conclusions	37
Recommendations	37
Bibliography	40
Appendix A: Space Environment Services Center Forecast	45
Appendix B: Algonquin Videometer Scan and Calibration Levels	46

Appendix C: SOON Card Format	49
Appendix D: SOON Program	53
Appendix E: Coordinate Transformation	61
Appendix F: Data Analysis Programs	66
Vita	69

List of Figures

<u>Figure</u>		<u>Page</u>
1	Prediction Hierarchy	2
2	Solar Observing Optical Network	8
3	Brightness Area Scan of an Active Region . . .	9
4	Algonquin Solar Drift Scan - 14 May 1978 . . .	24
5	Scattergram of CALSCN versus SOONAREA	29
6	Scattergram of NEWSN versus NEWAREA	32
7	Algonquin Solar Drift Scan - 1 May 1978 . . .	47
8	Format for Region Identifier Records	50
9	Format for Histogram Records	51
10	SOON Histogram Format - Card Image	52
11	Frame Orientations	61
12	Rotation About Y	62
13	Rotation About x	62
14	Spherical to Rectangular Coordinate Transformation	63

List of Tables

<u>Table</u>		<u>Page</u>
I	Sample SOON Program Printout - 14 May 1978 . .	24
II	Calibration Levels	48

lambda
ABSTRACT

→ Using a statistical regression model, a relationship was found between the area of solar active regions (bright in hydrogen-alpha, $\lambda = 6562.8 \text{ \AA}$ in the visible) and their 10.7 cm radio emission. Data used in this analysis were the brightness-area histograms obtained from the Solar Observing Optical Network (SOON) and daily drift scans obtained from the Algonquin Radio Observatory, Ottawa, Canada. This data, for the period 1 May through 15 July 1978, was used to develop the following relationship:

$$\text{Algonquin Scan Peak Value} = .88782838 + .00025237604 (\text{Calibrated SOON Area})$$

with a correlation coefficient, r , of .88509. Future models for predicting the 10.7 cm solar flux are theorized based on the established relationship.

C

CORRELATING RADIO EMISSIONS WITH VISIBLE EMISSIONS FROM
INDIVIDUAL SOLAR ACTIVE REGIONS

I. Introduction

Background

A definite correlation exists between hydrogen-alpha active regions on the sun and the 10.7 cm solar radio flux observed at 1700Z daily at the Algonquin Radio Observatory, Ottawa, Canada (Refs 7:454 and 8:126). Since this correlation has been shown, officers at the Solar Forecast Center, Air Force Global Weather Central (AFGWC), Offut Air Force Base, Nebraska, want to predict the actual 10.7 cm flux from observations of active regions with the Solar Observing Optical Network (SOON). Indeed, one of the ancillary purposes of this research will be to determine the feasibility of using SOON data as an input to a predictive model. The primary purpose of this research, however, will be to find a relationship between the Algonquin drift scans of the sun and the data from the SOON network. The SOON network has only existed since 1977, and to date little of the data has been used for any research purposes (Ref 38). The underlying rationale for this study is found in an article by Covington, Legg, and Bell describing the relationship between hydrogen-alpha filtergrams and west drift scans of the sun (Ref 9:471-473). Instead

of using hydrogen-alpha filtergrams, this data is replaced with the SOON data which is also centered on the hydrogen-alpha wavelength ($\lambda = 6562.8 \text{ \AA}$).

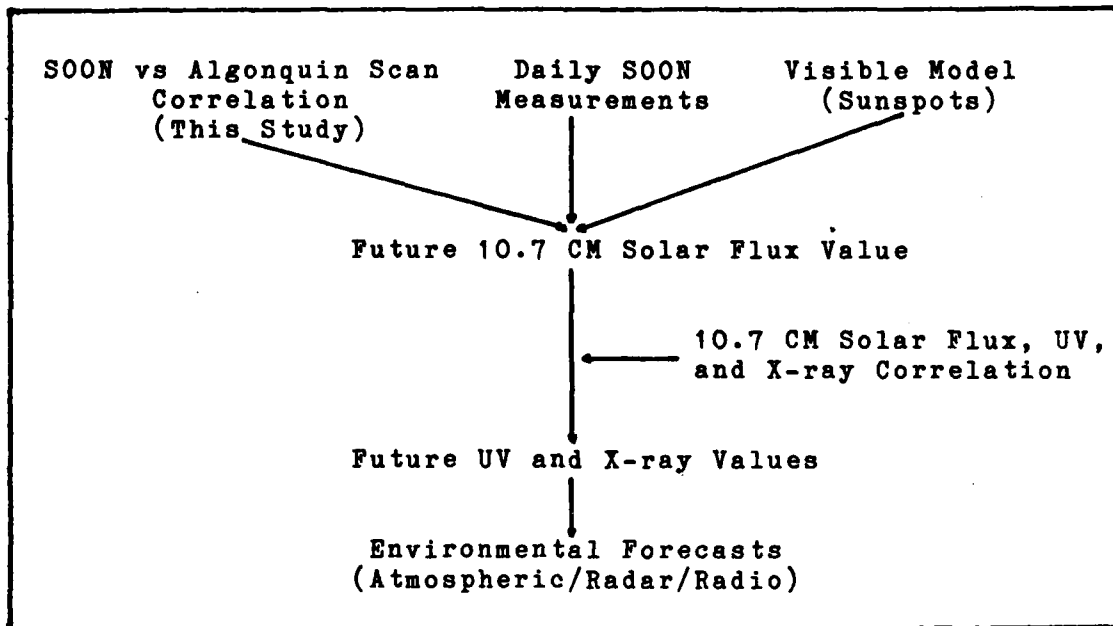


Figure 1. Prediction Hierarchy

Knowing active region area and sunspot activity, forecasters want to develop an accurate way of predicting the 10.7 cm flux from these features when they reappear after rotating out of the field of view of the earth. This involves roughly a 13-day lead-time depending on the region's latitude. Such a time development model of visible active regions would rely heavily on the proposed relationship being investigated by this study as well as current models of sunspot movement, development, and decay. These components could be synthesized into a predictive routine for the 10.7 cm solar flux with roughly a 13-day lead-time.

Prediction of the 10.7 cm flux is not the end product; rather, it is used as an indicator of solar ultraviolet (UV) and X-ray radiation. There is a documented correlation between the 10.7 cm radio flux, solar UV and solar X-ray radiation (Ref 11:2). The 10.7 cm flux is used as a predictor for these latter two radiations because 10.7 cm data can be collected on the ground whereas UV and X-ray measurements must be done above the atmosphere. Being able to predict the 10.7 cm flux in advance would allow similar lead-time prediction of UV and X-ray wavelengths. Of primary interest are the effects of UV and X-ray radiation on the earth's upper atmosphere. These include the density of the upper atmosphere which determines the drag experienced by low altitude satellites. Also, UV and X-ray radiation affects the structure and conditions of the ionosphere. Many agencies are very concerned with ionospheric effects because of the way they influence radar and radio transmissions. Figure 1 highlights these inter-relationships.

Now, with these factors in mind, a relationship must be developed between the SOON data and Algonquin Radio Observatory drift scans of the sun which can be used in future studies to predict the 10.7 cm flux using SOON data. This involves exploring growth and decay trends expected in the size of bright active regions from one day to the next, how the rotation of the sun affects apparent area of these regions at the earth due to foreshortening, viewing position (accounting for inclination of the earth's orbital plane and tilt of

the solar axis), latitudinal affects on the sun itself, and if the active region is above or below the solar equator. The above considerations can be gleaned from brightness-area histograms from the SOON network. The histograms are recorded daily for selected active regions on the sun. All of the above factors can be roughly accounted for based on a composite of the individual histograms.

Statement of the Problem

Data concerning the relationship between hydrogen-alpha active regions and the total solar 10.7 cm radio flux has existed since 1977, but no work has been done to relate these two data bases in the short term on a region by region basis. Most studies, none involving SOON data, deal with longer periods such as a month and the 11 year solar cycle.

Objective of the Research

The objective of this research will be to develop a relationship between SOON data and Algonquin drift scans which can be used as the basis for a forecast model for the 10.7 cm radio flux using brightness-area histogram scans from the SOON network. Basic hypotheses involved concern whether or not the SOON data is related to the Algonquin scans and whether it is significant enough to be used as a predictive tool.

Methodology

The objective of this study will be accomplished by analyzing data comprised of SOON brightness-area histograms

and 10.7 cm radio flux data from the National Oceanic and Atmospheric Administration (NOAA), Boulder, Colorado, and Algonquin Radio Observatory, respectively. The histograms and solar scans, though taken at different locations, are done at roughly the same time and can therefore be compared directly. A regression model will be developed with the data. The model will be run with the help of SPSS (Statistical Package for the Social Sciences) regression packages and the CYBER 1700 computer.

Limitations

As with any new system, SOON has some inherent limitations. In the preliminary stages of this research, it was hoped that digitized pictures of the solar disk would be available for analysis. This, however, was not the case. The sun is divided into regions for SOON observation, and all are not looked at daily. In fact, the SOON data available is limited to active regions on any given day. This means that the entire solar surface will not be available for analysis every day, and that a composite of available histogram data will have to be used to formulate a crude solar image for comparison with the solar scan data. Additionally, there are some gaps in the data due to cloudy weather conditions at the SOON and Algonquin sites and days when observations could not be made because of technical difficulties (Refs 4 and 30). For active regions near the limbs of the sun, large errors are introduced into the histogram data if the dark background sky

is included in the measurements. Data is generally recorded for regions as they move across the entire solar disk but is most accurate for those regions lying 65°E and 65°W of the central meridian (Ref 4). Therefore, most of the data from the solar limbs will have to be eliminated.

With these limitations in mind, the research was further constrained by the availability of the SOON data itself. Since the system is relatively new, little use has been made of the data. Because of this, most of the data is in raw form, requiring much time and effort to reduce to a usable form (brightness-area histograms). To date, the only available SOON data in reduced form covers the period from May 1978 to December 1978. This data base must be further reduced since only data corresponding to the 1700Z Algonquin drift scans is relevant. Therefore, of the available data taken throughout the day, only the readings (histograms) as close to 1700Z as possible for each region observed, will be used in this study. Unfortunately, there is one further problem. Mr. Arnold Star, Detachment 4, 3rd Weather Wing, Holloman AFB, one of the observer/collectors of the SOON data, informed me that he had serious doubts as to the validity of the data for this period in its present histogram form. Mr. Star feels that the data for the May 1978-December 1978 period may not be standardized. As he explained, a videometer is used to break the image into 64 shades of gray. The pixels in each band are then counted and equated to an area. The greatest number of counts should be centered on the background level to obtain a

normalized quiet sun level. Early readings (including the May 1978-December 1978 period) were not all normalized to the same quiet sun level. Some were normalized to 10 and some to 12 (on a 0-64 scale). Mr. Star suggested that the data be further normalized to account for all of these effects (Ref 39). This exercise is beyond the scope of this study. Instead, the data will be used as is. More accurate correlations and predictions will have to be the result of future studies in this area using later data that is more standardized.

One other obvious limitation with this technique is the time involved in getting the data into a usable format. For short-term predictions, the speed with which the data is processed and made available for analysis will have to be greatly increased. Otherwise, the SOON data will be of little practical value for short term predictions.

There are no readily apparent problems with the 10.7 cm solar flux data from the Algonquin Radio Observatory. This data has been used as a basis for prediction of the 10.7 cm solar flux since 1947. It has been the standard basis for all models with earth-based parameters (Ref 11:2).

II. Historical Survey

SOON Data

The Solar Observing Optical Network is one of the newest means by which solar related data can be collected on hydrogen-alpha active regions. This worldwide system was developed and is operated by the United States Air Force (USAF) Air Weather Service. As of now, there are four sites designed to collect data. Data collection began at Holloman AFB, New Mexico, in November 1977 and was soon supplemented by data from Palehua, Oahu, Hawaii, December 1977, Ramey, Puerto Rico, February 1979, and Learmonth, Australia in 1979. A fifth site has been proposed for somewhere in the Middle East.

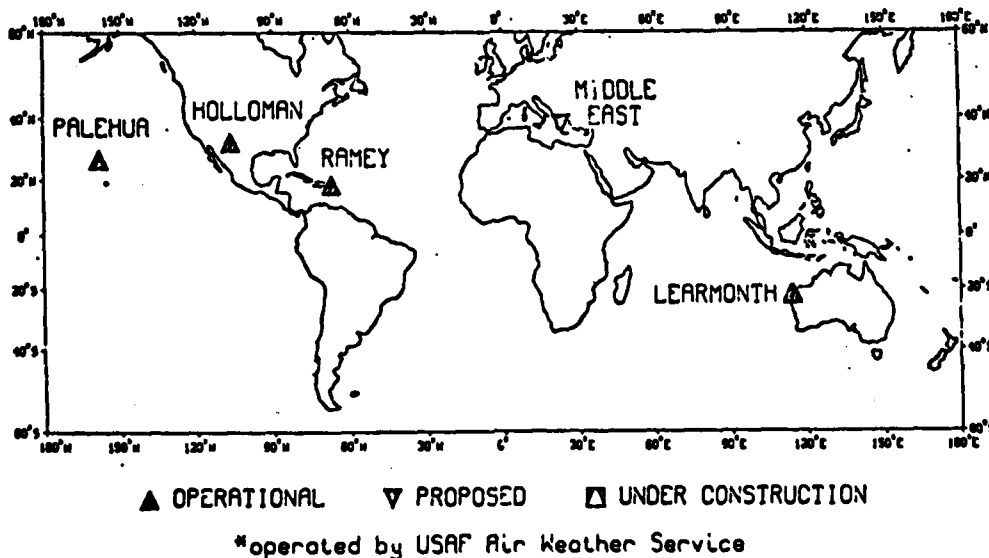


Figure 2. Solar Observing Optical Network (Ref 4)

The observing schedule of active regions at each observatory is decided upon by the duty observer, with suggestions from the parent site at Holloman, depending on the level and type of activity and the needs of real-time services; this determines the order of data on magnetic tape and companion photographic film.

As the system is so new, extensive work is still being done to determine how best to use all of the data. As uses are developed, more and more of the data will be processed into the final outputs, which consist of brightness-area histograms (see Figure 3), flare time-histories, as well as

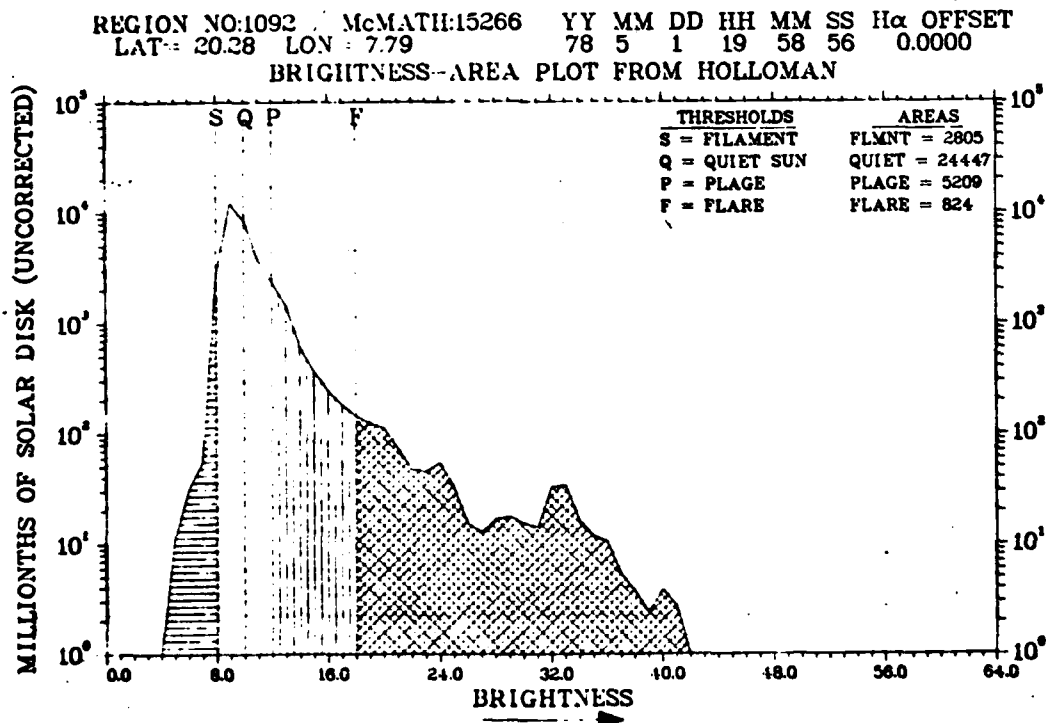


Figure 3. Brightness-area scan of an active region (Ref 30:1)

photographs of the corresponding solar phenomena. The brightness-area histogram depicted in Figure 3 is a graphical representation of all the data provided in each SOON histogram record set. Each record set could be used to construct a histogram in this form. The system is calibrated such that if the quiet sun mode occurs in bin 10 (bin equals 0-64), bin 20 is twice as intense and bin 30 is three times as intense. Borrowing from the SOON descriptive pamphlet:

The basic SOON telescope is a 25-cm evacuated refractor mounted on a polar axis using a monochromatic filter (0.5A bandpass) centered on the Hydrogen-alpha absorption line of the solar spectrum. A built-in minicomputer totally directs the collection of all data.

The digital H-alpha brightness-area data are the major data product from a SOON telescope. These data present brightness versus area information from particular flare-producing regions on the sun. The brightness ranges from dark shades, indicating relatively cool absorbing plasma, to very bright shades indicating hot emitting plasma, i.e., flares. Sixty-four shades of brightness are graphically presented on the horizontal axis of the brightness-area plot. The height of a brightness column represents the uncorrected area of a given brightness shade summed over the entire region. The observer sets threshold values for filament, quiet sun, plage, and flare according to observing conditions, and the corresponding areas in millionths of the solar disk (not corrected for foreshortening) are calculated and recorded on this plot. The automated capability of the SOON telescope system allows brightness-area information to be collected from as many as six regions per 5-sec interval. The system is usually programed to collect 1 to 3 brightness-area scans per minute from each selected region (Ref 30).

The 10.7 CM Solar Radio Flux

Radio emissions from the sun range from 8 mm to 15 m in wavelength of which the 10.7 cm wavelength (2800 MHz) is only a part (Ref 3:189). This band is essentially blackbody radiation from high temperature regions and varies slowly between fairly narrow limits (Ref 28:30). Also, part of the 10.7 cm radio flux is emitted by spiraling electrons in the sun's magnetic field and is sensitive to the strength of the magnetic field so that active regions with strong magnetic fields may emit stronger in the 10.7 cm radio flux than older less active regions (Ref 13:21). These radio emissions are made up of three components;

a fairly constant basic component (quiet sun emission), occasional bursts of different types and durations, closely associated with solar flares, and a slowly varying component...exhibiting roughly a 27-day recurrence period (Ref 10:734).

The basic component can be found by

plotting the apparent temperature vs projected sunspot area and extrapolating to zero sunspot area...the slowly varying component arises from regions at a height of 100,000 km above the photosphere and [is] associated with chromospheric faculae (Refs 3:189 and 35:223).

This has been verified since, as the sun rotates and varied size spots and spot groups move across the solar disk, the slowly varying component varies accordingly. Thus, the slowly varying component shows a close association with sunspot number and exhibits the 27 day variation (Ref 35:225).

Basically then, research indicates that, over and above the background basic component, the slowly varying component of the 10.7 cm radio flux is emitted from the corona and has a

10.5 year period associated with it (Refs 11:1,8;6:31;8:129; and 28:33). Often, the three components described above are not broken out in this manner. Only two components are discussed, active and background (Ref 1:3232).

With these regions and components in mind, a brief discussion will be made of the methods used and values obtained for the solar flux. The antennas used to obtain the radio flux are of low resolution so that the antenna beam covers the whole solar disk and the values obtained represent an average over the solar disk (Ref 15:4). These values have ranged from 67×10^{-22} Watts/m²/Hz to 380×10^{-22} Watts/m²/Hz (Watts/m²/Hz=Watts m⁻²Hz⁻¹=Jansky) since 1947 (Ref 36:Section 5,1) never falling below 65×10^{-22} Watts/m²/Hz (Refs 11:4 and 8:127). Richards has noted that "the values may differ by as much as 100 [$\times 10^{-22}$ Watts/m²/Hz] from one day to the next near their maximum, and generally by no more than 6 or 10 [$\times 10^{-22}$ Watts/m²/Hz] near their minimum values" (Ref 36:Section 5,1).

The 1700Z radio measurements for this study were obtained from the Algonquin Radio Observatory, Ottawa, Canada, with the cooperation of Mr. Aunri Gagnon. The drift curves are taken with a multi-element interferometer capable of providing multiple fan beams, 1.5' of arc east-west by 2° north-south, sufficiently separated so that only one response falls on the sun at any one time. When this is used in conjunction with an offset grating of four elements, a compound interferometer results capable of achieving a single-lobed fan beam with 15" arc east-west (Ref 9:465-466). This resolution produces scans

like the one depicted in Appendix B (Figure 7) which is representative of all the Algonquin data. The peaks represent radio emissive regions associated with plages and active regions.

10.7 CM Solar Radio Flux Uses

The 10.7 cm solar radio flux data, having the advantages of being measured on the earth's surface and for the longest period, are being used in many ways. Because of its long history of careful observation (Ref 19:327) and its use as a general predictor of solar radiation in Extreme Ultraviolet (EUV) and X-ray wavelengths (Refs 19:327;18:10; and 11:2), the 10.7 cm flux has evolved as a well-entrenched parameter that is used by a large number of radio communicators and upper atmospheric modelers for a variety of operational applications (Refs 19:327;14:1-2; and 8:131).

Usefulness. Descriptions of the usefulness of this parameter range from it being an excellent predictor of solar activity (Ref 28:33) to an opinion by one expert that its time has passed (Refs 12 and 13:21) and new and better methods should be adopted for more accurate prediction. Richards, commenting on the 10.7 cm flux, went as far as to say that "the yearly mean is all that can be reasonably predicted since the shorter period fluctuations are quite irregular and follow no pattern" (Ref 36:Section 5,1).

Predicted Values. There are similar feelings concerning the spectrum that the 10.7 cm flux is used to predict. In

regard to EUV, many scientists feel that the ten-centimeter flux is

too gross a parameter to accurately evaluate the state of the ionosphere and upper atmosphere and that more specific measurements in the EUV would improve the operational models. However, the lack of a consistent and on-going EUV observational program and the expense and disruption of redoing present operational models (Ref 19:327)

precludes eliminating the ten-centimeter flux as a model input. Until the advent of routine exoatmospheric EUV and X-ray satellite measurements, the 10.7 cm flux was seen as a fairly accurate predictor of these events (Ref 28:33). Now, however, since such measurements are more routine, numerous studies point out that the 10.7 cm flux is not a very accurate predictor at all (Refs 19:327;1:3231;12; and 13:21) and should not be relied upon for accurate ionospheric, upper atmospheric, and satellite drag models. Certain correlations are very good such as the one between the 10.7 cm flux and atmospheric density changes resulting from heating (Ref 1:3231) but this is an aggregate effect over a relatively long period. Whenever 10.7 cm flux data is smoothed, it generally gives a fairly good correlation in the long term but short term correlations are very poor (Refs 23:1;13:22). In this regard, there are documented effects due to solar rotation and whether measurements are taken near solar maximum or minimum (Ref 1:3231).

When dealing specifically with UV, Donnelly points out that:

sunspot number and 10.7 cm solar radio flux are useful as a general guide to the level of solar activity. However, they are not precise indications of the solar UV flux.

They can give very erroneous UV estimates when they are used for particular days rather than for average effects (Ref 13:21).

He goes on to say that

the 10.7 cm radio flux and sunspot number are of course correlated with the solar UV flux because all three are generally related to the number and size of active regions. The more smoothing applied to the data, the higher the correlation because the differences due to CMD [Central Meridian Distance] and magnetic field orientation and strength distribution among active regions become smoothed out to average values (Ref 13:22).

Such correlations are also found when 10.7 cm flux and flares are considered. Mohler has shown that the 10.7 cm daily flux provides a general guide to flare activity but that the accuracy varies for different flux levels (Ref 29:2). The same general finding applies to the correlation between the quiet sun soft X-ray flux and the 10.7 cm radio flux as investigated by Gibson and Van Allen (Ref 18:8-10). Finally, Bossy and Nicolet use the 10.7 cm flux as an input for their predictive model of Lyman-alpha irradiance (Ref 2:907).

From the foregoing survey, it can be surmised that better predictors are available with documented validity. They will eventually work their way into various predictive routines. But, until their data bases are significant and continuously recorded, as the Ottawa 10.7 cm flux data, their usefulness will be limited.

10.7 CM Solar Radio Flux Predictive Models

A result of the relative newness and lack of processing of the SOON data, coupled with numerous conversations with officials directly involved with collecting and processing the

data, it is clear that no one has attempted to develop a prediction scheme for the 10.7 cm solar flux using the SOON data (Refs 4;17; and 22). There have, however, been numerous other predictive techniques developed to predict the 10.7 cm flux in the long (up to a year), medium (month), and short term (days). By using SOON data, forecasters hoped to eliminate some of the observer dependent subjectivity associated with existing 10.7 cm prediction methods.

Cautions. The relationship between the Zurich relative sunspot number, plage index, and the 10.7 cm flux has been established and used by many scientists to predict the 10.7 cm flux (Ref 7:454 and 8:126). A brief review of efforts from the long to short term follows some appropriate cautions from Yu I. Vitinskii, an expert in solar activity forecasting. Vitinskii points out that any prediction based on sunspots and sunspot areas suffers from inherent inaccuracy due to visibility conditions and limb effects. Atmospheric conditions and proximity of spots to the solar limbs add a great deal of uncertainty to the number and area of spots. If these parameters are used in prediction models, the output is less than optimum since errors are compounded. This is one reason monthly and yearly values are preferred so the values can be smoothed to reduce inaccuracies (Ref 42:5). Vitinskii's observation related to these long term techniques is often quoted: "we have shown that the reliability of the results obtained using these methods still leaves much to be desired" (Ref 42:103).

Long Term Techniques. The extensive effort of Slutz et al is an example of using smoothed Zurich 13 month mean sunspot numbers to predict the 10.7 cm solar flux. This study was supposed to be an aid in solar activity prediction by first developing a model to predict sunspot numbers several years in advance and then use these values to predict the corresponding 10.7 cm flux value. An integral part of the study was therefore to determine which of several mathematical expressions best described the relationship between the 10.7 cm flux and the Zurich 13 month mean sunspot number. The results indicated that a second order equation was acceptable to represent the relationship over the 12 month period since, up to the time of the study, little consideration had been given to this relationship for periods less than one-half of a solar cycle (1 cycle is approximately 11 years) (Ref 37:87). The long-term technique advocated in this study was considered valid enough to be used as the 10.7 cm flux prediction method in NASA's Solar Activity Prediction of Sunspot Numbers (Ref 24:1) and its subsequent verification (Ref 32). Note, however, that this model and its applications are used in the long term for the 13 month smoothed 10.7 cm flux value and do not impact on the present study.

Some atmospheric density and satellite drag modelers have also evolved their own methods for predicting the 10.7 cm flux as well as other parameters needed in their models. Richards developed a piece-wise linear model for different levels of the smoothed sunspot number (R_z):

$$0 < R_z < 30 \quad \bar{F}_{10.7} = 68 + 0.60R_z \quad (1)$$

$$30 < R_z < 70 \quad \bar{F}_{10.7} = 60 + 0.825R_z \quad (2)$$

$$70 < R_z < 200 \quad \bar{F}_{10.7} = 50 + .967R_z \quad (3)$$

where $\bar{F}_{10.7}$ is the yearly mean flux value (Ref 36:Section 5,2). Slutz' colleagues, Stewart and Leften, compared the results from their final second order equation for predicting the yearly mean 10.7 cm flux value (ξ_{12})

$$\xi_{12} = 63.7451 + 0.728015R_{12} + .000890443(R_{12})^2 \quad (4)$$

with Richard's equations values and found the results to be very similar (Ref 37:107). Again, the long term nature of these studies negate their usefulness for short term predictions.

As discussed by Gibson and Van Allen, Kraus determined two components of the 10.7 cm flux in his book Radio Astronomy (Ref 26:Chapter 3). He showed that the radio flux density at earth from an optically thin emitting region is

$$P = 2.7 \times 10^{-48} T^{-1/2} S \quad (5)$$

where P is the radio flux density at 10.7 cm at 1 Astronomical Unit in units of 10^{-22} Watts $(m^2 Hz)^{-1}$, T is the electron temperature in 10^6 K, and $S = \int N_e^2 dV$, the volumetric emission measure in cm^{-3} (N_e is the electron number density in cm^{-3} and dV is the element of volume in cm^3) (Ref 18:15). The volume integral is taken over the emitting region, assumed to be at the same temperature T throughout. For an optically thick

emitting region

$$P = 1.1 \times 10^{-19} AT \quad (6)$$

where A is the projected area in cm^2 of the outer surface of the emitting region as viewed from earth (Ref 18:16). These equations were developed using data from a limited period where P ranged from $90.1 \leq P \leq 261.7$. It seems as though these equations could be used in the short term depending on variable availability, but this was never done on a regular basis.

Medium Term Techniques. Jack Slowly at the Smithsonian Astrophysical Observatory developed the following relationship for use by NOAA to predict the monthly flux based on the smoothed Zurich relative sunspot number 13 month average. This technique uses a least-square regression model to generate the predicted smoothed \bar{R}_{13} values which are then used as inputs to linear regression equations to compute $\bar{F}_{10.7(13)}$ solar flux values (Refs 19:332 and 16:380)

$$\bar{F}_{10.7(13)} = 49.4 + 0.97\bar{R}_{13} + 17.6\exp(-0.035\bar{R}_{13}) \quad (7)$$

This equation was used by Holland, Rhodes, and Euler to extend values of the 10.7 cm flux back to 1749 in order to develop a predictive model of solar activity (Ref 23:2).

Short Term Techniques. For short term predictions, forecasters at the Global Weather Central initially used a regression technique to establish a trend based on the last 3 solar rotations (weighted toward the most recent rotation) and

the trend for the past two or three days of the current rotation. Then, using the east-west 10.7 cm scans from the National Research Council, Ottawa, to establish the relative location of radio plages and thereby estimate the effects of solar rotation, they varied their prediction based on experience (Ref 19:341 and 22). This procedure may lack rigor but until that time provided the only very short term forecast of 10.7 cm flux (see Appendix A for sample output) (Ref 28:48).

The most rigorous models used for predicting smoothed values for the 10.7 cm flux and geomagnetic indices are SUNSPOT developed by the NASA Marshall Space Flight Center, the Air Force Global Weather Central 27-day regression forecast subroutine, and EST10 developed by NOAA. SUNSPOT is used for statistical estimation of future expected values of the monthly 10.7 cm solar flux and the 5 month smoothed flux values ($F_{10.7}$) (Ref 41). The AFGWC 27-day regression forecast subroutine predicts the 10.7 cm solar flux for the 27 days following the current day's 10.7 cm flux (Ref 22). EST10 is used to estimate the 10.7 cm flux value for 1, 2, and 3 days into the future. It must be continually updated and run in order for the short term forecasts to be accurate. To date, this is the most refined short term predictive tool. In fact, it virtually ignores any long term effects and produces very subjective results since the operator can change the inputs based on his experience (Ref 22). As with each of the other models, these procedures do not rely on any SOON data inputs.

III. Methodology

Data Reduction

Before the data could be used, it had to be reduced into formats for comparison. The Algonquin data, in graphic form, of solar scans, could be used for direct comparison with the SOON data. The scans are taken of the sun from the west limb to the east over a period of about two to four minutes daily at 1700Z (Ref 9:465 and 27:749). See Appendix B for an example. The scans are of the apparent sun without correcting for the solar tilt in relation to the ecliptic (P angle) or the heliocentric location of the sun's center (B_0 and L_0). These angles did have to be considered when trying to make a direct comparison with the SOON data since P, B_0 , and L_0 are accounted for in the region identification of this data. For the purpose of this analysis, P, B_0 , and L_0 were considered constant for the entire day. In the ephemeris they are for 0000Z whereas they are used for corrections to measurements taken at 1700Z (Ref 40:350-353). Small variations produced by this difference were not considered significant.

Each brightness-area histogram from the SOON network has a specific format (See Appendix C). The first card of a four or eight card sequence (single or double length histogram, respectively) has all the identifying information for the particular region being examined and calibration data for

being able to relate each histogram record to the others. Since, on a given day, in the time frame of interest (near 1700Z), the SOON instrument can sample numerous regions many times each, the optimum approach was to average the data for each region observed. The SOON program was written for this purpose. This program not only averages the daily readings near 1700Z for each region observed, but also corrects the region area to account for foreshortening (See Appendix D) and performs a coordinate transformation on the original SOON latitude and longitude to get the data points in the reference frame of the Algonquin data (Ref 25:8-13). See Appendix E for a derivation of the transformation algorithm used. This transformation allows for direct comparison of the SOON bright regions with the bright region peaks on the Algonquin scans and provides a rough idea of the location of the region in terms of solar radii distance from the central meridian. This is done with a spherical to rectangular coordinate transformation (Ref 34:35-38).

In order to validate the SOON program, a sample set of data was selected to exercise the various aspects of the program. As with the real data, it allowed for summing the areas above the quiet sun level for a rough approximation of activity in each region measured, selecting the appropriate daily P , B_0 , and L_0 readings from the ephemeris, deciding whether a single or double length histogram was being read (column 1 of card 10), reading the region identifier, day, time, latitude, longitude, wavelength offset, quiet sun level,

and calibration constant. Most of these features are then used in the program to obtain summary data or as checks to determine if the data set should be discarded (for example, a wavelength offset other than zero causes the histogram to be purged; wavelength offset gives an indication of how far from the hydrogen-alpha centerline the readings are. If it is not zero, additional corrections must be made to the readings which were beyond the scope of this study). After accounting for all of these factors, the data was in a form for direct comparison.

Data Comparison

Now, having summary data by each method, a comparison was made region by region for each day to determine if bright regions on the SOON scans corresponded to bright areas (in longitude only) on the Algonquin plots. Since the Algonquin data can only give an indication of the relative distance of active regions from the solar central meridian, a rough comparison of longitudes is possible but not pinpoint accuracy in either latitude or longitude. This becomes apparent when looking at the Algonquin scans. In reality then, the latitude reading produced by the SOON program is unnecessary but is included for completeness.

As previously mentioned, available data from the SOON network was limited to the May to December 1978 time frame. Of this, only data from 1 May through 16 July 1978 could be used in the analysis. Additional data was unavailable due to

the time and expense involved in processing it.

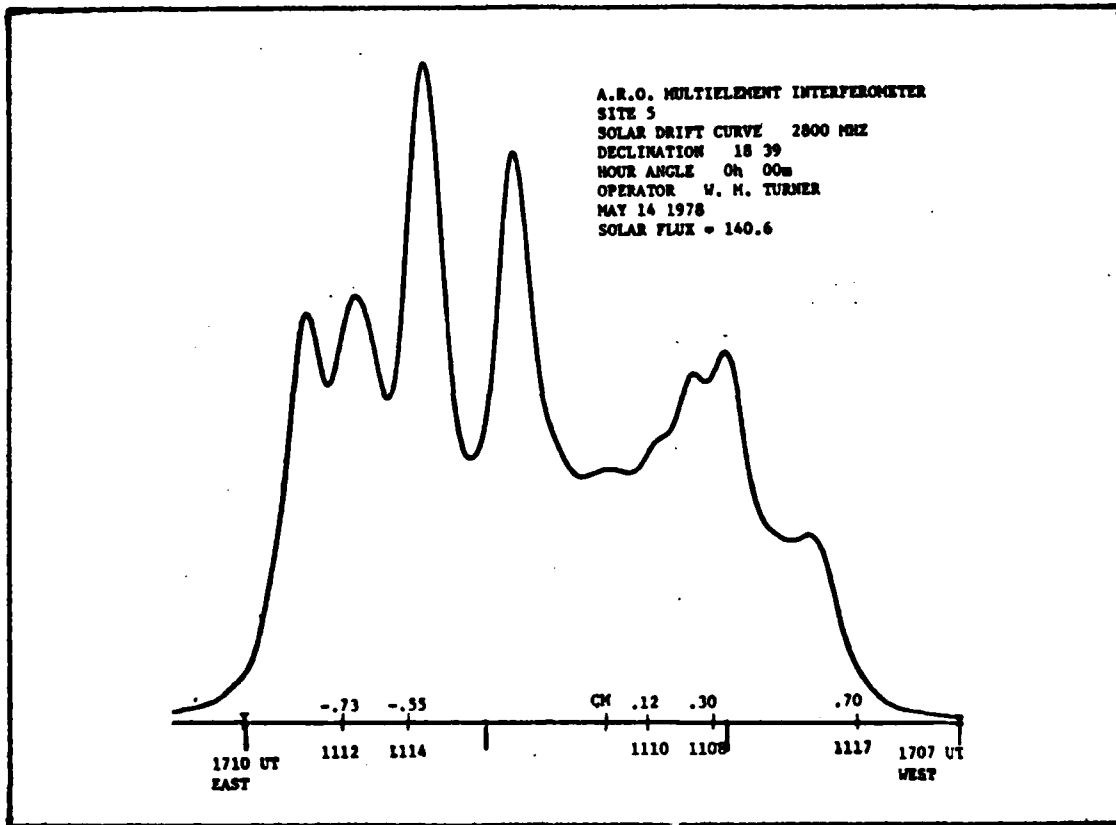


Figure 4. Algonquin Solar Drift Scan - 14 May 1978

Table I

Sample SOON Program Printout - 14 May 1978

SUMMARY TABLE FOR DATE: 780514 IS:										
REGION	LAT	LONG	TOTAL AREA	OBSV	AVG AREA	COR AREA	NLAT	NLONG	SOLRAD	
1114	-26.81	-68.79	10700.55	9.	1188.95	2602.25	-46.31	-53.26	-.55	
1110	-19.65	-1.26	38982.68	9.	4331.41	4527.33	-21.28	7.38	.12	
1117	-22.52	39.53	49449.53	9.	5496.61	7527.70	-10.03	45.27	.70	
1099	27.37	81.65	4048.81	9.	451.15	899.04	8.52	85.04	.99	
1112	21.54	-44.23	37916.19	9.	4212.91	6522.73	4.30	-46.73	-.73	
1108	17.19	26.24	12900.85	9.	1433.43	1703.35	22.96	19.08	.30	

Figure 4 and Table I will help in understanding the methodology involved. This data set is typical of all the data reviewed. The solar drift curve is a reduction of the

actual curve received for 14 May 1978. The east and west solar limbs are identified by the tick marks labeled 1710 UT and 1707 UT, respectively. The USAF numbered regions and percentage of solar radii for each, identified by the SOON data, are also shown. CM is the approximate location of the central meridian. The summary table for 14 May 1978 is representative of the output from the SOON Program. It identifies the USAF numbered regions observed each day (REGION), their latitude and longitude in the heliocentric frame of the sun (LAT and LONG), total area of all histograms of the same region (TOTAL AREA), number of histograms recorded for each region (OBSV), the average area for the region observed (AVG AREA), the average area corrected for foreshortening (COR AREA), the new latitude and longitude in the Algonquin reference frame (NLAT and NLONG), and the percent of solar radius where each region lies in reference to the solar central meridian (SOLRAD).

One notable characteristic is the second highest spike on the Algonquin plot just to the east of the central meridian. Throughout all of the scans that tracked this feature across the sun, there was never a corresponding SOON region that could be matched with it. This is to be expected since there are some features detected by one method that may not have a match in the other data. Based on scans that came before this one, the various spikes on the Algonquin plot could be correlated with active regions identified by the SOON data. Note that Region 1099 was eliminated immediately since its

longitude was far beyond the 65 degree limit and resulted in an apparent solar radius of greater than 90 degrees. In comparing the above data sets it is apparent that the SOON data indicates large bright areas at 73 and 55 percent of a solar radius east of the central meridian and 12, 30, and 70 percent of a solar radius west of the central meridian. To arrive at the locations on the 10.7 cm radio drift scan plot for these points, the distance between the indicated east and west limbs was divided in half, and these percentages were applied to this figure. This procedure was considered reasonable since the SOON data was unitized to solar radii by setting $R_{\odot} = 1.0$ as described in Appendix E. As theorized, spikes corresponding to each of these identified regions exist on the Algonquin plot.

This method of rough comparison substantiates the existence of a correlation which appeared between a majority of the daily scans and SOON summary printouts. From the data on successive days, a given active region could be tracked across the sun at roughly the correct solar rotational velocity for the region's latitude (Ref 17:31). The fact that both the Algonquin scans and SOON data depicted this movement further reinforces the existence of a relationship between the phenomena. A point to remember about the Algonquin data is that, due to the sensitivity of the equipment, it must be adjusted to keep each day's reading from being too great. Therefore, if a very bright region is in the scan, the gain must be reduced to keep that region within the bounds of the

equipment. When the active region rotates out of the field of view of the instrument and the instrument gain is increased, specific features may become apparent that had been obscured.

The calibration constants in Appendix B (Table II) make all the 10.7 cm drift scan readings comparable and were applied before data analysis. This was done by measuring the peak in centimeters (scale not important) corresponding to an active region identified by the SOON equipment. The values obtained were then divided by the calibration constant for the day under study to arrive at the numerical input from the Algonquin data that would be compared with its corresponding region area as defined by the SOON data.

Data Analysis

Once both data sets were reduced to this point, they were in a form for direct comparison to determine if a relationship existed between them with the hope of finding a definite mathematical relationship. If such a relationship could be established, it could then be used for developing more accurate forecasting models of the 10.7 cm solar flux. This then, is the major aspect of this study; to determine if a relationship exists between the irradiance of the active regions identified by the SOON data and the features identified by the Algonquin plots. To attempt to establish this relationship, the magnitude of the Algonquin plot peak values corresponding to active SOON regions were measured as mentioned previously. The SOON corrected areas made up the other

half of the data. Areas were used since they represent the relative brightness of each region above the quiet sun level that correspond to active regions on the Algonquin plots. All told, there were 180 data points (individual features in both the Algonquin and SOON data) available. These represented 53 distinct USAF numbered regions in a two and a half month period. Of these, 38 SOON data points and their corresponding Algonquin plot values had to be discarded because they were too far into the solar limbs (greater than 80 degrees east or west of the solar central meridian). Even though three of the data points had longitudes greater than 65 degrees, they were left in because they were only slightly greater than 65 degrees.

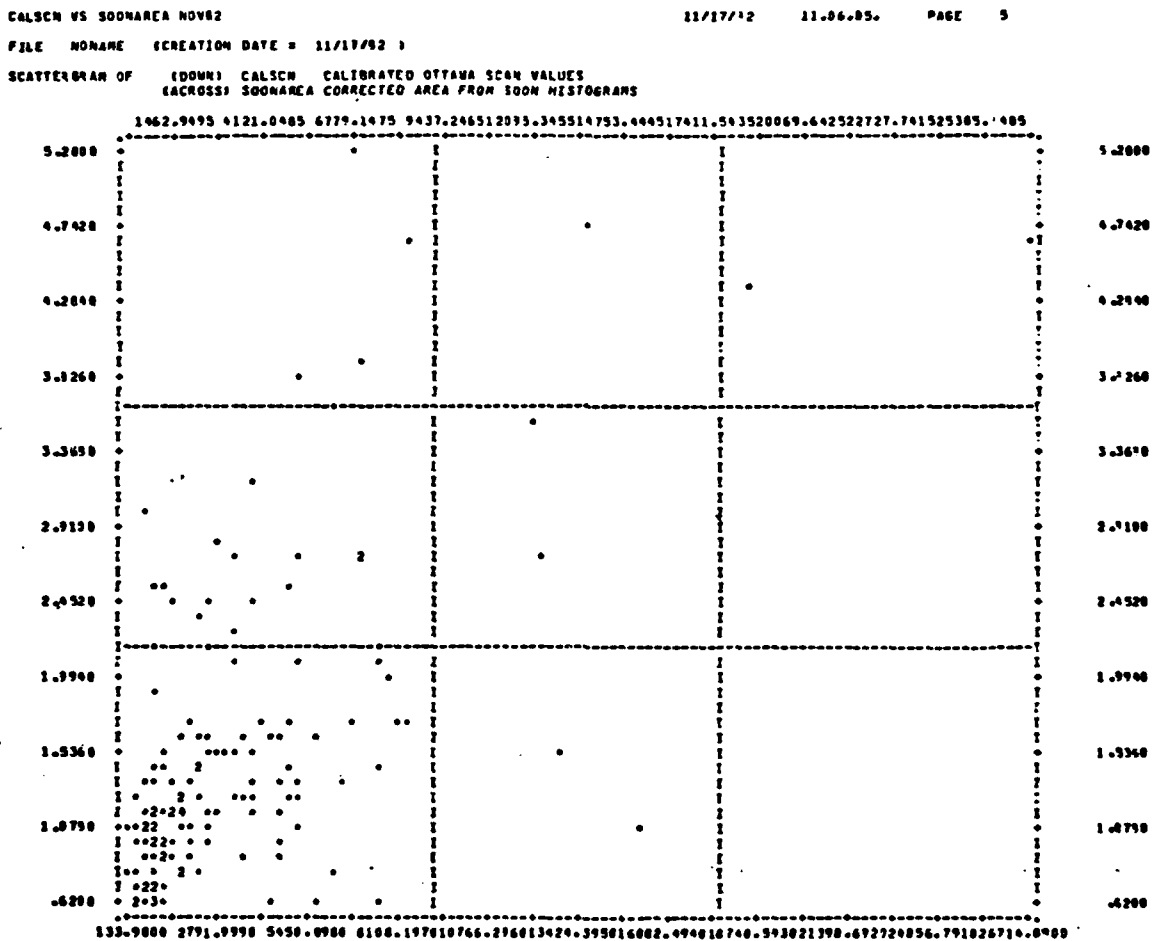
Model Development

The final pairing resulted in 142 points for input into the data analysis programs (see Appendix F). Though more would have been desired, this sample should be enough to validate or refute the existence of a relationship between the SOON and Algonquin data. Since there was only one feature from each of the data sets, a simple linear regression routine was used to compare the data (Ref 5:1-22 and 33:320-349, 293-300). The basic linear regression model used was

$$Y = a + \beta X + \epsilon \quad (8)$$

where a and β are the intercept and slope, respectively, and ϵ is the random error with mean zero and variance σ^2 . The model further assumes:

1. The sample is random,
2. The dependent variable, Y (Algonquin scan value), is drawn from a normal distribution for any given value of X (corrected area from SOON),
3. The regression of X and Y is linear,
4. All of the Y values have the same variance, and
5. The random errors, ϵ_i , are independent of each other.



CALSCN VS SOONAREA NOV82 11/17/92 11.06.95. PAGE 5

Figure 5. Scattergram of CALSCN versus SOONAREA

The first attempt at a regression equation relating X and Y was apparently unsuccessful. The scattergram plot of the data seen in Figure 5 does not indicate any substantial relationship between SOON area and Algonquin intensity. The mathematical formula determined gives even less hope of a relationship:

$$\text{CALSCN} = B (\text{SOONAREA}) + A \quad (9)$$

or

$$\text{CALSCN} = .00015 (\text{SOONAREA}) + 1.09429 \quad (10)$$

where

CALSCN = calibrated Algonquin scan value, and

SOONAREA = corrected area from the SOON histograms.

The correlation coefficient, r , was equal to .59932 with an r^2 of .35919. The correlation coefficient indicates how well a regression line characterizes the linear relationship between two variables while r^2 is a measure of the proportion of variance in one variable explained by the other and measures the strength of the relationship between the two variables (Ref 33:279).

At this point, it seemed reasonable that a better mathematical relationship could be found. Relying on techniques described by Neter and Wasserman (Ref 31:131-136), the plot depicted in Figure 5 seemed to indicate that the variance increases as X (SOONAREA) increases. Therefore, using their

technique for cases in which the standard deviation of the error terms in the regression equation is proportional to X, the following transformations were developed:

$$Y' = Y/X \quad (11)$$

$$X' = 1/X \quad (12)$$

so that

$$Y' = \alpha + \beta X' + \epsilon \quad (13)$$

becomes the basic equation. In the two analysis programs, Equations (11) and (12) become

$$\text{NEWSCN} = \text{CALSCN}/\text{SOONAREA} \quad (14)$$

and

$$\text{NEWAREA} = 1/\text{SOONAREA} \quad (15)$$

When these values were used in the SPSS regression routine a better correlation was established as shown in the scattergram in Figure 6. From this, the resulting equation for predicting an active region on the Algonquin scans with SOON data is:

$$\text{NEWSCN} = B (\text{NEWAREA}) + A \quad (16)$$

which, in the variables of interest, becomes

$$\text{CALSCN}/\text{SOONAREA} = B (1/\text{SOONAREA}) + A \quad (17)$$

FILE NO NAME CREATION DATE = 11/17/82

SCATTERGRAM OF (SOON) NEWSCH
(ACRCS) NEWAREA

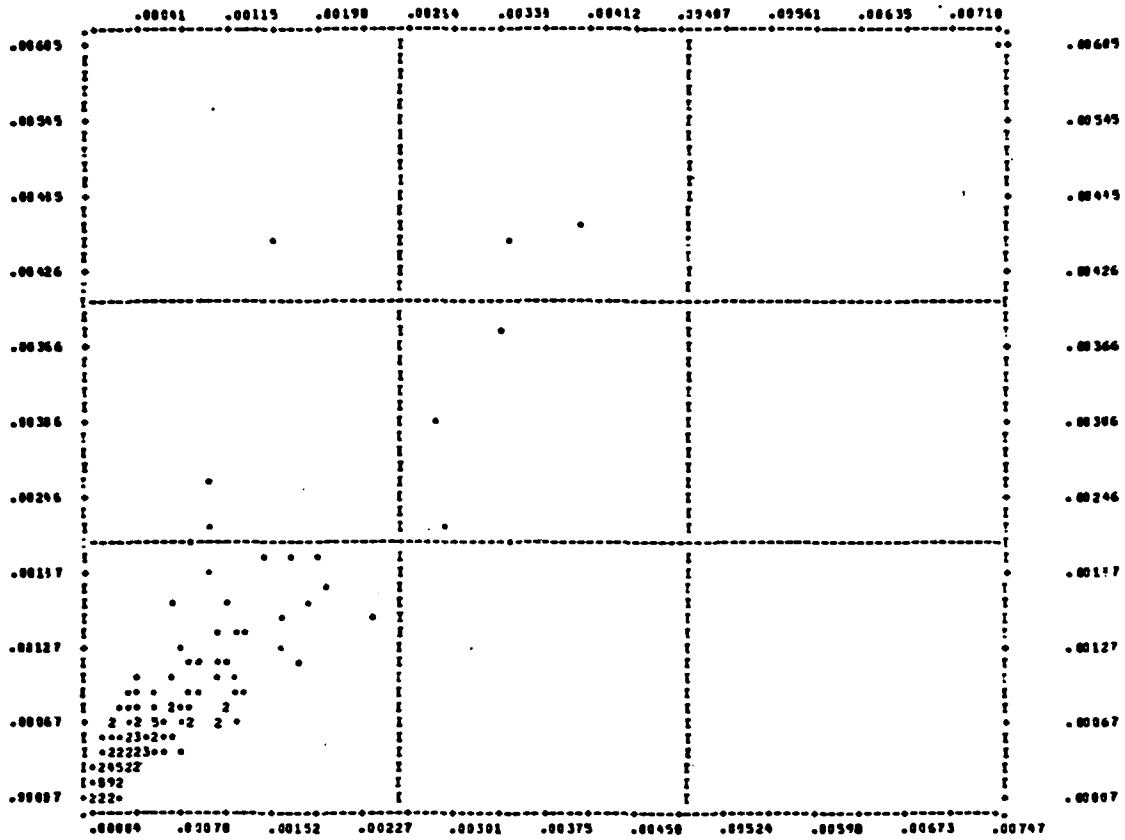


Figure 6. Scattergram of NEWSCH versus NEWAREA

The correlation coefficient for this relationship is .88509 giving an r^2 of .78338 which indicates that the regression equation defines a good relationship between the dependent (calibrated Algonquin scans) and independent (SOON corrected area) variables. Equation (17) can be simplified to

$$CALSCN = B + A (SOONAREA) \tag{18}$$

resulting in

$$\text{CALSCN} = .88782838 + .00025237604 (\text{SOONAREA}) \quad (19)$$

using the statistics provided in the SPSS program.

Confidence Interval

Equation (19) is good for point estimates but because the deviations from the line increase with large SOONAREA, the certainty associated with the point estimate becomes less for large SOONAREA. Therefore, in order to quantify the potential errors involved in using this equation, confidence limits must be established. The 95 percent prediction interval for values predicted with Equation (19) is found as follows (Ref 21:373-374):

$$\begin{aligned} \hat{Y}_0/X - t_{\alpha/2, n-2} \sqrt{\text{MSE}' [1 + 1/n + (X' - \bar{X}')^2 / S_{XX}']} &\leq Y_0/X \\ &\leq \hat{Y}_0/X + t_{\alpha/2, n-2} \sqrt{\text{MSE}' [1 + 1/n + (X' - \bar{X}')^2 / S_{XX}']} \end{aligned} \quad (20)$$

where

$\hat{Y}_0/X = Y_0'$ = NEWSKN value predicted using Equation (16),

\hat{Y}_0 = CALSCN value predicted using Equation (19),

X = SOONAREA observed,

Y_0 = The true value of CALSCN,

$t_{\alpha/2, n-2} = t_{.05/2, 140} = 1.97$,

MSE' = Mean square error of the transformed data,

X' = Transformed X value for which CALSCN value is to be predicted,

\bar{X}' = Mean of transformed X values, and

S_{xx}' = Corrected sum of squares of X of the transformed X values = $(n-1)(s_x'^2)$

which results in a confidence interval in terms of the original data of

$$\begin{aligned} \hat{Y}_0 - t_{\alpha/2, n-2} \sqrt{MSE' [1 + 1/n + (X' - \bar{X}')^2 / S_{xx}']} X &\leq Y_0 \\ \leq \hat{Y}_0 + t_{\alpha/2, n-2} \sqrt{MSE' [1 + 1/n + (X' - \bar{X}')^2 / S_{xx}']} X &\quad (21) \end{aligned}$$

with

$$MSE' = .00019012 ,$$

$$\bar{X}' = .0007445 , \text{ and}$$

$$S_{xx}' = 141 (.0009306)^2 = .0001221083 ,$$

so the confidence interval becomes

$$\begin{aligned} \hat{Y}_0 - 1.97 \sqrt{.00019012 [1 + 1/142 + (X' - .0007445)^2 / .0001221083]} X &\leq Y_0 \\ \leq \hat{Y}_0 + 1.97 \sqrt{.00019012 [1 + 1/142 + (X' - .0007445)^2 / .0001221083]} X &\quad (22) \end{aligned}$$

Equation (22) verifies that the width of the interval increases as X increases which corresponds to what is observed in the original data.

Equations (19) and (22) are consistent with the five assumptions expected of a linear regression model. The results indicate the sample was random, the dependent variable, Y, came from a normal distribution for any given value of X, and, after the transformation, the regression was linear, the

variation of Y was constant, and the random errors were independent.

Other Relationships

After reviewing the residual analysis performed on the data by the analysis program (See Appendix F), it seemed that at least one outlying data point may have been unduly influencing the regression equation. All together, there were six residuals greater than two standard deviations. These represented about five percent of the total and were expected, however, one point (CALSCN = 3.04, SOONAREA = 668.29) had a residual twice as great as the next largest residual. After rechecking the data reduction for this point and finding nothing wrong, it was decided to explore the effects of this point on the regression equation. The point was eliminated from the data and the programs were rerun. Equations (11) through (18) still apply only now the resulting equation is:

$$\text{CALSCN} = .869333787 + .00024499284 (\text{SOONAREA}) \quad (23)$$

which resulted in an r of .91565 and r^2 of .83842 on the transformed equation. The confidence limits for values predicted with this equation are:

$$\hat{Y}_0 - 1.97 \sqrt{.00012736 [1 + 1/141 + (X' - .0007391)^2 / .0001215552]} \leq Y_0$$

$$\leq \hat{Y}_0 + 1.97 \sqrt{.00012736 [1 + 1/141 + (X' - .0007391)^2 / .0001215552]} \quad (24)$$

which has a derivation similar to Equation (22). Even though the linear association between the dependent and independent

variables, as measured by the correlation coefficient, is better than the original formulation, there is no valid reason to exclude the data point in question other than the fact that it is not typical of the rest of the data. For this reason, the model defined by Equations (19) and (22) is the best relationship found between the Algonquin scans and the SOON data. Note also that even with the point removed, Equation (23) does not differ appreciably from Equation (19).

To further explore the correspondence between the Algonquin scan values and the SOON data, a second set of data was developed from the original histogram records. Now, however, absolute brightness was calculated for each SOON region by multiplying each area by its bin value (relative brightness). Since each bin is linearly brighter than the preceding one, this should give a good indication of how active the region is. This means that the larger a bin area is, the greater its contribution to the overall brightness of the region which, in turn, should be reflected by a larger spike in the corresponding Algonquin scan. As expected, similar results were obtained with this method as in the first analysis and will not be pursued further here.

IV. Conclusions and Recommendations

Conclusions

From this analysis it is apparent that a relationship does exist between Algonquin drift scans of the sun and SOON histogram records of active regions on the sun. The area above the quiet sun level calculated from the SOON data can be used to predict the location and intensity of solar bursts in the 10.7 cm solar radio range as gleaned from the Algonquin scans of the sun. With further analysis, as recommended below, the SOON histograms could become a valuable tool in aiding the understanding of the relationship between solar active region area and the 10.7 cm solar flux.

Recommendations

In order to improve this analysis several important modifications to this experiment could be done to refine the results.

1. The ephemeris data used in the analysis could be modified to account for the fact that the tabulated values are for 0000Z while the Algonquin solar scans and SOON records were taken at 1700Z each day. Though these changes are small, at certain times of the year the angles do vary rapidly and could affect the accuracy of the data.

2. To use as much data as possible, corrections could be applied to those SOON data records with a wavelength offset

other than zero. Though few records have a wavelength offset other than zero, those that do could be significant and should not be wasted.

3. Further discussions with the SOON engineers and physicists might uncover better ways to categorize and quantify the histograms. In this study, the quiet sun value was used as a benchmark to determine what brightness levels (bin numbers) should be summed to get a rough idea of a region's brightness above the background value, thus making an inference as to the region's contribution to hydrogen-alpha wavelength, and, after regression, 10.7 cm flux. A better benchmark might be found such as using the flare threshold rather than brightness above quiet sun.

4. Data used in any follow on study must be standardized. The only data available for this study was in the May-December 1978 time frame. The SOON system was very new at the time and was going through considerable growing pains. This is reflected in the fact that data was not all standardized to the same quiet sun level (some was "standardized" to bin 10 while some was "standardized" to bin 12). If the same time frame is used, the data must all be standardized to the same level.

5. Though the Algonquin scans are supposed to be taken at 1700Z, they often slip one way or the other by as much as 20 minutes. Since the SOON data was only available at 1700Z, if this was the case, the data was compared as if both readings were taken at 1700Z. In the future, the times of both data sets should be matched exactly.

6. A study such as this might be expanded to try and find a relationship between SOON data and other wavelengths. Such studies would involve other SOON sites besides just Holloman, New Mexico.

7. In the future, data must be analyzed for a longer period. Though data from May through December 1978 was available, not all of it could be used. Future studies should expand to cover many months (6 or more) and even years rather than just 2 1/2 months, especially when many days are lost to weather and equipment problems. Additionally, as many regions as possible should be included each day. Finally, studies should explore any relationship between the solar cycle and these results, looking specifically at periods during solar maximum and solar minimum.

8. A more complex method should be investigated for determining the intensity of the Algonquin data than measuring the peak values. One possibility is to take an average value for each active longitude (as identified by a spike). Another would be to integrate the area under the curve.

9. Analysis should be done to perfect methods to predict the 10.7 cm solar flux using the Algonquin solar scans. Once this is done, based on the present study, SOON data could be used to predict the 10.7 cm solar flux.

Bibliography

1. Anderson, Albert D. "Long-Term (Solar Cycle) Variation of the Extreme Ultraviolet Radiation and 10.7 Centimeter Flux from the Sun," Journal of Geophysical Research, 70:3231-3234 (July 1965).
2. Bossy, Lucien and Marcel Nicolet. "On the Variability of Lyman-Alpha with Solar Activity," Planetary and Space Science, 29:907-914 (August 1981). (81A48711).
3. Brandt, John C. and Paul W. Hodge. Solar System Astrophysics. New York: McGraw-Hill Book Co., Inc., 1964.
4. Buhmann, Ronald W. SOON Data Manager (private communication). NOAA/EDIS, D64, Boulder, Colorado. August 1982.
5. Cohen, Claude, et al. Manual Number 414 (Rev C). SPSS Regression Reference. SPSS Updated Regression Procedures. Evanston, Illinois: Vogelback Computing Center, Northwestern University, July 1978.
6. Covington, Arthur E. "A 10.5 Year Period for the Slowly Varying Component of the Solar Radio Flux," Royal Astronomical Society of Canada Journal, 68:31-35 (February 1974). (74A24667).
7. -----"Solar Noise Observations on 10.7 Centimeters," Proceedings of the Institute of Radio Engineers, 36:454-457 (April 1948).
8. -----"Solar Radio Emission at 10.7 CM, 1947-1968," Royal Astronomical Society of Canada Journal, 63:125-132 (1969).
9. Covington, Arthur E., T. H. Legg, and M. B. Bell. "A High Resolution 2800 MHZ Multi-Element Interferometer," Solar Physics, 1:465-473 (1967).
10. Das Gupta, M. K. and S. K. Sarkar. "Recurrence of 10.7 CM Solar Flux and of Sunspot Activity over the 11-Year Solar Cycle," Indian Journal of Pure and Applied Physics, 8:734-735 (November 1970). (71A22792).

11. Donnelly, Richard F. "Comparison of Nonflare Solar Soft X-ray Flux with 10.7 CM Radio Flux," Unpublished paper. National Oceanic and Atmospheric Administration, Environmental Research Laboratories, Boulder, Colorado, 1982.
12. -----Solar Forecaster and Atmospheric Modeler (private communication). NOAA/Environmental Research Laboratories, Boulder, Colorado, July 1982.
13. -----"Variations in Solar UV Spectral Irradiance and X-ray Flux," Proceedings of the Symposium on Solar Terrestrial Influences on Weather and Climate, edited by Billy M. McCormac. Boulder, Colorado: Colorado Associated University Press, 1982.
14. Donnelly, Richard F. and J. H. Pope. The 1-3000 Å Solar Flux for a Moderate Level of Solar Activity for Use in Modeling the Ionosphere and Upper Atmosphere. NOAA Technical Report ERL 276-SEL 25. Boulder, Colorado: Department of Commerce, National Oceanic and Atmospheric Administration, August 1973. (74N2933).
15. El-Raey, Mohamed and Philip Scherrer. Differential Rotation in the Solar Atmosphere Inferred from Optical, Radio, and Interplanetary Data. Technical Report 71 Series 12 Issue 77. Berkeley, California: University of California, Berkeley, Space Sciences Laboratory, 1971. (AD 731-403).
16. Euler, Harold C., et al. "MSFC Solar Activity Predictions for Satellite Orbital Lifetime Estimation," Solar Terrestrial Predictions Proceedings, Vol I, Prediction Group Reports, 378-384, edited by Richard F. Donnelly. Boulder, Colorado: Department of Commerce, National Oceanic and Atmospheric Administration, August 1979. (80N18492).
17. Gibson, Edward G. The Quiet Sun. Washington, D. C.: National Aeronautics and Space Administration, Scientific and Technical Information Office, 1973.
18. Gibson, Jean and James A. Van Allen. Correlation of X-ray Radiation (2-12 Å) with Microwave Radiation (10.7 cm) from the Non-Flaring Sun. Report Number University of Iowa 70-5-Revised. Iowa City, Iowa: University of Iowa Department of Physics and Astronomy, April 1970.
19. Heckman, Gary R. "Predictions of the Space Environment Services Center," Solar Terrestrial Predictions Proceedings, Vol 1, Prediction Group Reports, 322-349, edited by Richard F. Donnelly. Boulder, Colorado: Department of Commerce, National Oceanic and Atmospheric Administration, August 1979.

20. -----Forecaster, Space Environment Services Center, National Oceanic and Atmospheric Administration, Environmental Research Laboratories (private communication). Boulder, Colorado, July 1982.
21. Hines, William W. and Douglas C. Montgomery. Probability and Statistics in Engineering and Management Science (Second Edition). New York: John Wiley and Sons, 1980.
22. Hirman, Joseph W. Chief Forecaster, Space Environment Services Center, National Oceanic and Atmospheric Administration, Environmental Research Laboratories (private communication). Boulder, Colorado, July 1982.
23. Holland, Robert L., et al. Lagrangian Least-Squares Prediction of Solar Activity. NASA Technical Memorandum 82462. Marshall Space Flight Center, Alabama: George C. Marshall Space Flight Center, April 1982.
24. Johnson, Gordon G. and Samuel R. Newman. Shuttle Program Solar Activity Prediction of Sunspot Numbers, Predicted Radio Flux. NASA-TM-81109, JSC-16390, Report-80-FM-8. Houston, Texas: Mission Planning and Analysis Division, Lyndon B. Johnson Space Center, NASA, February 1980. (80N28286).
25. Kaplan, Marshall H. Modern Spacecraft Dynamics and Control. New York: John Wiley and Sons, 1976.
26. Kraus, John D. Radio Astronomy. New York: McGraw-Hill Book Co., 1966.
27. Legg, T. H. , M. B. Bell, and R. C. Bignell. "Observations of Intense Radio Sources with a 1'.5 Fan Beam," The Astronomical Journal, 73:749-755 (November 1968).
28. Magnis, Stephen J. Introduction to Solar Terrestrial Phenomena and the Space Environment Services Center. NOAA Technical Report ERL 315-SEL 32 Boulder, Colorado: Department of Commerce, National Oceanic and Atmospheric Administration, January 1975.
29. Muhler, Orren C. Final Report - Relationships Between Solar Flares and Other Aspects of Solar Activity - For the Period October 1, 1966 - September 30, 1971. Project Number 013-205, ORA-085980. Ann Arbor, Michigan: University of Michigan Department of Astronomy, November 1971. (AD732469).

30. National Geophysical and Solar-Terrestrial Data Center (D63). Solar Activity Data From SOON Network. Description of data available. Boulder, Colorado: Department of Commerce, National Oceanic and Atmospheric Administration, 1979.
31. Neter, John and William Wasserman. Applied Linear Statistical Models. Homewood, Illinois: Richard D. Irwin, Inc., 1974.
32. Newman, Samuel R. Shuttle Program. Solar Activity Prediction of Sunspot Numbers (Verification), Predicted Solar Radio Flux, Predicted Geomagnetic Indices A and K_p. NASA-TM-81139, JSC-16762, Report-80-FM-41. Houston, Texas: Mission Planning and Analysis Division, Lyndon B. Johnson Space Center, NASA, August 1980. (80N31297).
33. Nie, Norman H., et al. Statistical Package for the Social Sciences (Second Edition). New York: McGraw-Hill Book Company, 1975.
34. Protter, Murray H. and Charles B. Morrey, Jr. Modern Mathematical Analysis. Reading, Massachusetts: Addison-Wesley Publishing Company, 1964.
35. Rao, D. R. K. "On the Spectral Study of Sunspot Number and Solar Radio Flux Between 600 and 9400 MHZ," Indian Academy of Sciences Proceedings, Section A, 73:223-231 (1971). (71A39324).
36. Richards, T. J. Final Report - Orbital Lifetime Studies, Section 5. HRED/112-1. Huntsville, Alabama: Lockheed Missile and Space Company, 17 December 1965. (A712549).
37. Slutz, R. J., et al. Solar Activity Prediction. NASA-CR-1939. Boulder, Colorado: Department of Commerce, National Oceanic and Atmospheric Administration, November 1971. (N72-12807).
38. Springer, Bruce D. Air Force Representative, Environmental Research Laboratories, Short Term Predictions, National Oceanic and Atmospheric Administration (private communication). Boulder, Colorado, July 1982.
39. Star, Arnold. Solar Forecaster, Detachment 4, 3rd Weather Wing (private communication). Holloman AFB, New Mexico, August 1982.
40. The American Ephemeris and Nautical Almanac for the Year 1978. Washington, D. C.: U. S. Government Printing Office, 1976.

41. Vaughan, William W. Chief, Atmospheric Sciences Division, Space Sciences Laboratory, George C. Marshall Space Flight Center (private communication). Marshall Space Flight Center, Alabama, June 1982.
42. Vitinskii, Yu I. Solar Activity Forecasting. Translated from Russian, Israel Program for Scientific Translations, Jerusalem, NASA Technical Translation F-289. Springfield, Virginia: Clearinghouse for Federal Scientific and Technical Information, 1965. (N66-14135).

APPENDIX A

Space Environment Services Center Forecast

The following example is the primary forecast issued on 19 July 1974. Note the 10.7 cm forecast and 90-day mean in Section IV (Ref 28:49).

NNNN

KBOU

HFUS BOU 192200

FROM SPACE ENVIRONMENT SERVICES CENTER BOULDER COLO

SDF NUMBER 200

JOINT AFGWC/SESC PRIMARY REPORT OF SOLAR AND GEOPHYSICAL ACTIVITY ISSUED 2200Z 19 JULY 1974

IA. SOLAR ACTIVITY HAS BEEN VERY LOW WITH THREE NON-ENERGETIC SUBFLARES REPORTED DURING THE PAST 24 HOURS. REGIONS 438 (S08W72) AND 443 (SL2E06) HAVE BEEN STABLE. MINOR INTENSITY FLUCTUATIONS HAVE OCCURRED IN REGIONS 442 (SLOW34) AND 445 (S04W37). AN ACTIVE PROMINENCE (SL3E90) PARTIALLY ERUPTED, AND THEN TOTALLY DISSIPATED, BETWEEN 0715-0840Z. NO OTHER ACTIVITY HAS BEEN REPORTED TO SUBSTANTIATE AN ACTIVE RETURN OF OLD REGION 435.

IB. SOLAR ACTIVITY IS EXPECTED TO REMAIN LOW.

II. THE GEOMAGNETIC FIELD HAS BEEN QUIET. IT IS EXPECTED TO BE QUIET TO UNSETTLED.

III. EVENT PROBABILITIES 20 - 22 JULY

CLASS M 03/03/03

CLASS X 01/01/01

PROTON 01/01/01

PCAF GREEN

IV. OTTAWA 10.7 CM FLUX

OBSERVED 19 JULY 84

PREDICTED 20 - 22 JULY 83/85/85

90-DAY MEAN 19 JULY 90

V. GEOMAGNETIC A INDICES

OBSERVED FREDERICKSBURG 18 JULY 06

ESTIMATED AFR/AP 19 JULY 04/06

PREDICTED AFR/AP 20 - 22 JULY 07/08 - 09/10 - 11/12

SOLTERWARN

SPAN

BT

APPENDIX B

Algonquin Videometer Scan and Calibration Levels

The following videometer scan (Figure 7) is typical of the data received from the Algonquin Radio Observatory. These same scans are reproduced in Solar Geophysical Data (May 1978-July 1978) in a much smaller format. The east and west limbs of the solar disk are annotated on the graph and the point halfway between these points gives an approximate indication of the Central Meridian location. Based on this data, rough correlations with longitude could be made with active regions identified by the SOON data. The spikes on this graph represent longitudes with higher than normal activity. The horizontal baseline is for reference only and had to be adjusted slightly to standardize all of the plots. Adjustments took the form of adding or subtracting a small correction from the plot readings if the scan did not start precisely on the baseline. These readings were then further standardized by applying the daily calibration constants listed in Table 2.

MAY 1 1978

A.R.O. MULTIELEMENT INTERFEROMETER

SITE 5

SOLAR DRIFT CURVE 2800 MHz

DECLINATION $15^{\circ} 07'$

HOUR ANGLE $0^h 09^m$

OPERATOR P. Smith

SOLAR FLUX = 1785
3db atten

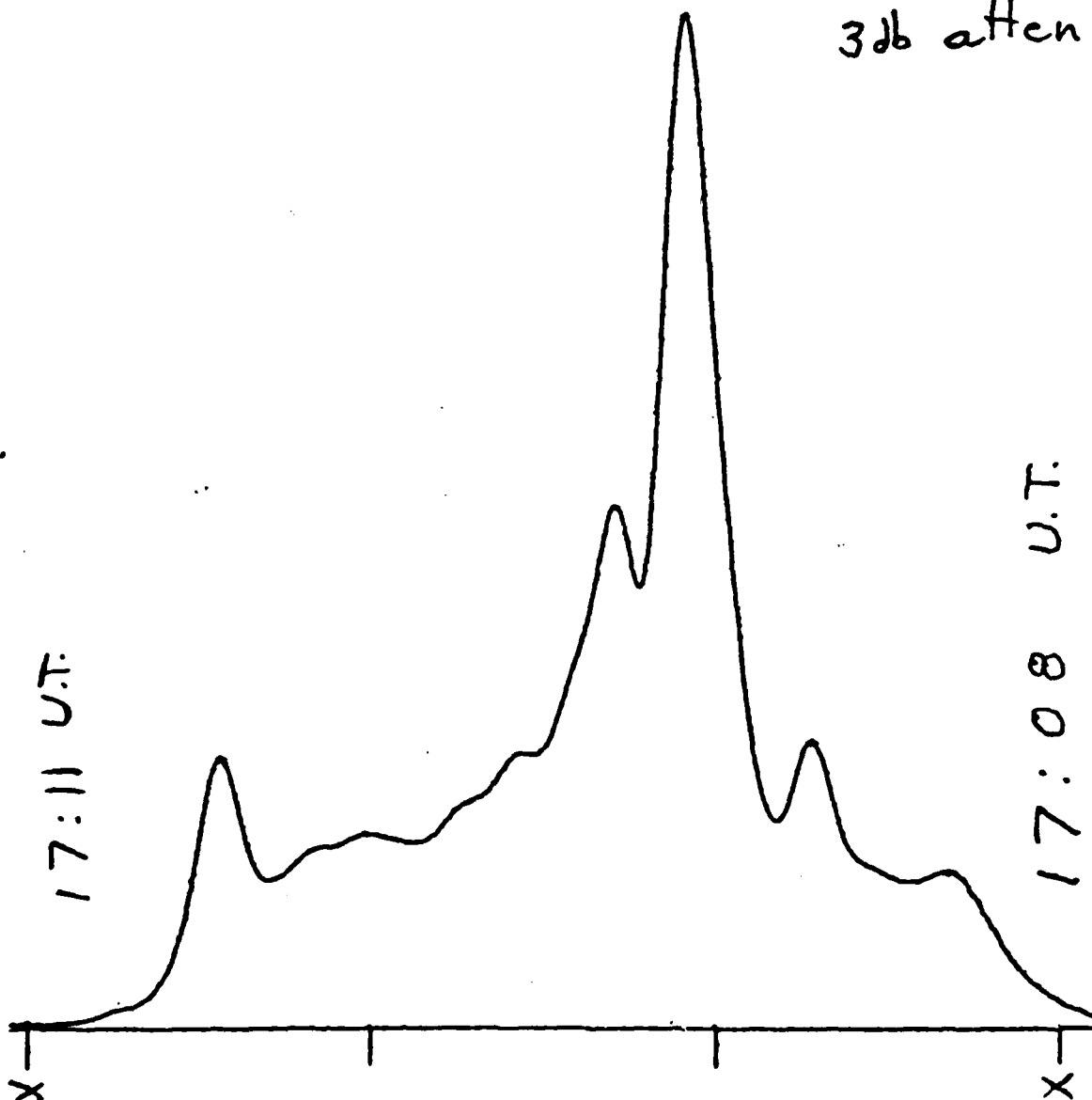


Figure 7. Algonquin Solar Drift Scan - 1 May 1978

Table II
Calibration Levels

	May	June	July	Aug.	Sept.	Oct.	Nov.	Dec.
1	3.15	6.16	4.99	5.71	3.09	5.59	5.45	5.05
2	3.04	5.93	5.53	5.41	2.99	5.87	4.99	5.23
3	3.18	6.37	5.79	5.60	3.04	5.53	4.71	6.23
4	3.19	6.19	5.71	5.38	3.11	5.27	4.26	5.51
5	3.03	6.37	5.87	5.74	3.01	5.56	5.33	4.67
6	3.01	5.86	5.60	5.77	2.87	5.87	5.45	5.19
7	2.81	6.05	5.56	5.81	2.77	5.56	4.73	5.44
8	2.76	5.92	5.84	5.62	2.94	5.61	4.38	5.89
9	5.84	NO DATA	5.70	5.96	2.82	2.66	4.30	2.13
10	5.86	4.73	2.83	6.02	2.87	2.53	4.47	2.13
11	5.43	6.02	2.68	5.72	5.73	2.64	4.45	1.37
12	6.00	5.98	2.80	5.72	5.68	4.39	4.38	2.71
13	6.10	5.44	2.74	5.66	5.81	4.90	5.05	2.40
14	6.29	5.92	2.79	5.51	5.87	5.26	4.04	2.50
15	5.80	6.05	2.68	5.27	5.85	5.13	4.21	2.20
16	6.06	5.99	2.77	5.08	6.19	5.51	4.60	2.32
17	6.21	5.81	2.77	5.47	6.08	5.45	4.80	4.98
18	5.84	5.97	2.70	5.61	6.10	5.33	4.47	5.20
19	5.86	5.95	2.28	5.75	3.00	4.93	4.20	5.57
20	6.38	5.42	5.57	5.18	2.97	5.38	5.33	5.25
21	6.25	6.03	5.28	5.74	2.80	5.35	5.94	4.54
22	NO DATA	5.52	5.61	5.64	6.21	5.30	5.05	5.31
23	6.27	5.67	5.66	5.79	2.93	5.19	4.95	5.07
24	2.78	5.74	6.19	5.61	2.88	5.24	5.65	5.21
25	5.83	6.73	5.97	5.48	2.86	4.56	4.69	5.26
26	6.19	2.79	5.06	5.75	3.32	4.48	NO DATA	2.46
27	6.15	6.19	5.90	5.91	2.86	4.70	4.83	2.53
28	6.32	5.76	5.67	6.15	2.71	4.12	4.98	2.47
29	5.99	5.66	5.65	6.00	2.81	4.96	4.97	4.85
30	6.15	5.54	6.26	2.85	5.63	5.14	5.07	5.53
31	6.59		6.03	6.00		4.36		5.28

APPENDIX C

SOON Card Format

The SOON data was received on punched cards. A region identifier record format is shown first. These cards are used by the SOON scientists to identify regions to be observed by the SOON telescopes and give region identifying information that is inherent in each of the histograms which follow for that region. Following this is the format for the SOON histogram data sets. The basic card layout is specified and then an example card image is presented. The SOON program outlined in Appendix D follows this format to reduce the data.

FORMAT FOR REGION IDENTIFIER RECORDS

COLUMN	PARAMETER	DESCRIPTION
1	ICONT	CONTINUATION CODE
2	NOBS	OBSERVATION CODE
3-6	IDENT	RGN # or RGDF
7-8	MTIME(1)	YEAR
9-10	MTIME(2)	MONTH
11-12	MTIME(3)	DAY
13-14	MTIME(4)	HOUR
15-16	MTIME(5)	MINUTE
17-18	MTIME(6)	SECOND
19-22	NIDRGN	NEW REGION IDENTIFIER
23-24	IRCHG	CHANGE
25-28	REGID	REGION IDENTIFIER
29-33	IRBITS	REGION CONTROL BITS
34-38	SLONG	REGION CENTER LONGITUDE (POS=WEST,NEG=EAST)
39-43	SLAT	REGION CENTER LATITUDE (POS=NORTH,NEG=SOUTH)
44-53	RV	BOX CENTER RADIUS VECTOR
54-63	SINPA	SINE OF THE P ANGLE FOR BOX CENTER
64-73	COSPA	COSINE OF THE P ANGLE FOR BOX CENTER
74-83	DLTLG	SOLAR ROTATION RATE AT THIS LATITUDE (RAD.)
84-88	SIZEEW	E-W SIZE IN VIDOMETER UNITS
89-93	SIZENS	N-S SIZE IN VIDOMETER UNITS
94-95	THRSHS	THRESHOLDS
96-97	THRSHQ	
98-99	THRSHP	
100-101	THRSHF	
102-106	AVBIN	AVERAGE BRIGHTNESS

Figure 8. Format for Region Identifier Records

FORMAT FOR HISTOGRAM RECORDS

***** CARD IMAGE RECORDS *****

<u>Card 10:</u> COLUMN	(1st card of sequence) PARAMETER	DESCRIPTION
1	ICONT	CONTINUATION CODE
2	NOBS	OBSERVATORY CODE
3-6	IDENT	REGION IDENTIFIER
7-8	MTIME(1)	YEAR
9-10	MTIME(2)	MONTH
11-12	MTIME(3)	DAY
13-14	MTIME(4)	HOUR
15-16	MTIME(5)	MINUTE
17-18	MTIME(6)	SECOND
19-23	SLAT	LATITUDE OF REGION CENTER (RADIAN)
24-28	SLONG	LONGITUDE OF REGION CENTER (RADIAN)
29-32	DLTWLJ	WAVELENGTH OFFSET (from H-alpha center)
33-36	SETUP(1)	STANDARD OPTICAL TV SETUPS
37-40	SETUP(3)	
41-44	SETUP(5)	
45-49	MODE2	STATISTICAL MODE OF SECOND READ
50-55	CAL	CALIBRATION CONSTANT
56-60	JNF	NUMBER OF FIELDS INTEGRATED
61	BLANK	
62-78	SORTKEY	DUPL OF COL 2-18 USED FOR SORTING ONLY...
79-80	CARD NO.	VALUE = 10

Figure 9. Format for Histogram Records

APPENDIX D

SOON Program

The following program reduced the SOON histogram inputs into a usable and comparable form. The data was received on punched cards in the format depicted in Appendix C. The hundreds of data records involved were run through the program and outputted in the tabular format described in the text. Comments are included in the program to document what is occurring at each point. Many of the operations performed may seem redundant but they were left in this format so each could be readily identified and as an aid to clarity. Appendix E contains a detailed explanation of the coordinate transformation used to get the data into a common reference frame.

```

100-CAP,CH70000,T100,I0120. T820740,PUZ,4172
110-FTN5.
120-LGO.
130-*EOR
140- PROGRAM SOON
150-CCCCCCCCCCCCCCCCCCCCCCCCCCCCCCCCCCCCCCCCCCCCCCCCCCCCCCCCCCCC
160-C THIS PROGRAM REDUCES THE SEMI-PROCESSED SOON DATA INTO C
170-C DAILY SUMMARIES OF SOLAR ACTIVE REGIONS. THESE REGIONS C
180-C WILL BE IDENTIFIED BY USAF REGION NUMBER, SOLAR LATITUDE C
190-C AND LONGITUDE BASED ON THE HELIOCENTRIC CENTER OF THE SUN C
200-C FOUND IN THE AMERICAN EPHEMERIS AND NAUTICAL ALMANAC-1978, C
210-C BRIGHT REGION AREA, AND REVISED LATITUDE AND LONGITUDE IN C
220-C THE REFERENCE FRAME OF THE ALGONQUIN DATA. C
230-C CAPT CRAIG A. PUZ AFIT/ENA GSO 82D 23 OCTOBER 1982 C
240-CCCCCCCCCCCCCCCCCCCCCCCCCCCCCCCCCCCCCCCCCCCCCCCCCCCCCCCCCCCC
250-C
260- INTEGER YRMODE,TIME,AREA,I,J,M,N,DATA(64),FLAG,FOUND,
270- +LPCNTR,YESTDY,EPHDAY,DAY,QBIN,QSUN,LA,LN,NOREG,WAVOFF,CAL1
280- REAL LAT,LON,PI,LOS,Z,
290- +ALFA(245,4),STORE(14,9),RAD,THETA,BO,LO,A,B,C,P,CAL
300- CHARACTER REGION*4,REGONS(14)*4
310-C
320-CCCCCCCCCCCCCCCCCCCCCCCCCCCCCCCCCCCCCCCCCCCCCCCCCCCCCCCCCCCC
330-C INITIALIZE ALL VARIABLES AND ARRAYS. EPHDAY SPECIFIES THE C
340-C NUMBER OF DAYS THE PROGRAM WILL RUN. IT MUST BE UPDATED C
350-C PRIOR TO EACH RUN. YESTDY IS THE DATE OF THE FIRST DATA C
360-C SET (YEAR/MONTH/DAY TWO DIGITS EACH). LAT AND LON ARE C
370-C THE LATITUDE AND LONGITUDE OF THE FIRST REGION SCANNED ON C
380-C ON THE FIRST DAY. C
390-CCCCCCCCCCCCCCCCCCCCCCCCCCCCCCCCCCCCCCCCCCCCCCCCCCCCCCCCCCCC
400-C
410- AREA=0
420- LPCNTR=0
430- YESTDY=780501
440- LAT=-481
450- LON=1266
460- PI=ACOS(-1.0)
470- RAD=2*PI
480- NOREG=0
490- EPHDAY=9
500-C
510- DO 3 I=1,64
520- DATA(I)=0
530- 3 CONTINUE
540-C
550- DO 20 I=1,14
560- REGONS(I)='
570- 20 CONTINUE
580-C
590- DO 7 I=1,14
600- DO 9 J=1,9
610- STORE(I,J)=0.0
620- 9 CONTINUE
630- 7 CONTINUE
640-C
650- DO 6 N=1,EPHDAY
660- DO 4 M=1,4
670- ALFA(N,M)=0.0
680- 4 CONTINUE
690- 6 CONTINUE
700-C

```

```

710-CCCCCCCCCCCCCCCCCCCCCCCCCCCCCCCCCCCCCCCCCCCCCCCCCCCCCCCCCCCC
720-C READ EPHEMERIS DATA IN TO AN ARRAY. P=POSITION ANGLE OF C
730-C THE NORTHERN EXTREMITY OF THE AXIS OF ROTATION OF THE SUN C
740-C MEASURED EASTWARD FROM THE NORTH POINT OF THE DISK. BO AND C
750-C LO=HELIOGRAPHIC LATITUDE AND LONGITUDE, RESPECTIVELY, OF C
760-C THE CENTER POINT OF THE SOLAR DISK. C
770-CCCCCCCCCCCCCCCCCCCCCCCCCCCCCCCCCCCCCCCCCCCCCCCCCCCCCCCCCCCC
780-C
790- DO 15 N=1,EPHDAY
800- READ(*,5) (ALFA(N,M),M=1,4)
810- 5 FORMAT(1X,F7.0,1X,F6.2,2X,F5.2,2X,F6.2)
820- 15 CONTINUE
830-C
840- DO 12 N=1,EPHDAY
850- WRITE(*,8) (ALFA(N,M),M=1,4)
860- 12 CONTINUE
870- 8 FORMAT(1X,F7.0,1X,F6.2,2X,F5.2,2X,F6.2)
880-C
890-CCCCCCCCCCCCCCCCCCCCCCCCCCCCCCCCCCCCCCCCCCCCCCCCCCCCCCCCCCCC
900-C READ FIRST CARD OF NEW DATA SET (HISTOGRAM). FLAG=1 OR 2 C
910-C SPECIFYING SINGLE OR DOUBLE LENGTH HISTOGRAM. YRMODE=YEAR, C
920-C MONTH, AND DAY OF HISTOGRAM. TIME=HOUR, MINUTE, AND SECOND C
930-C OF READING (NOT USED). LA, LN=REGION LATITUDE AND LONGITUDE C
940-C IN RADIANS (DIVIDED BY 1000 FOR ACTUAL READING). WAVOFF= C
950-C WAVELENGTH OFFSET (PROXIMITY OF READING TO HYDROGEN-ALPHA C
960-C CENTERLINE). HISTOGRAM IS DISCARDED IF THIS IS OTHER THAN C
970-C ZERO. QSUN=QUIET SUN BIN VALUE ON HISTOGRAM. AFTER C
980-C ROUNDING TO THE NEAREST INTEGER, ALL BINS ABOVE QSUN+2 ARE C
990-C ADDED AND REPRESENT THE RELATIVE BRIGHTNESS OF THE REGION. C
1000-C CAL1 IS A CALIBRATION CONSTANT. C
1010-CCCCCCCCCCCCCCCCCCCCCCCCCCCCCCCCCCCCCCCCCCCCCCCCCCCCCCCCCCCC
1020-C
1030- 1 READ(*,10,END=300)FLAG,REGION,YRMODE,TIME,LA, LN,WAVOFF,
1040- +QSUN,CAL1
1050- 10 FORMAT(11,1X,A4,2I6,2I5,I4,12X,I5,I6)
1060-C
1070-CCCCCCCCCCCCCCCCCCCCCCCCCCCCCCCCCCCCCCCCCCCCCCCCCCCCCCCCCCCC
1080-C CONVERT LATITUDE AND LONGITUDE TO REAL VALUES IN RADIANS. C
1090-C CONVERT CALIBRATION CONSTANT INTO REAL VALUE. C
1100-CCCCCCCCCCCCCCCCCCCCCCCCCCCCCCCCCCCCCCCCCCCCCCCCCCCCCCCCCCCC
1110-C
1120- LAT=REAL(LA)/1000.0
1130- LON=REAL(LN)/1000.0
1140- CAL=REAL(CAL1)/1.0E6
1150-C
1160-CCCCCCCCCCCCCCCCCCCCCCCCCCCCCCCCCCCCCCCCCCCCCCCCCCCCCCCCCCCC
1170-C COMPARE DATE ON LATEST CARD WITH PREVIOUS CARDS DATE. IF C
1180-C IT IS THE SAME, CONTINUE ADDING TO PRESENT DAY. OTHERWISE, C
1190-C IT IS A NEW DAY AND THE PREVIOUS DAY'S DATA MUST BE C
1200-C SUMMARIZED. C
1210-CCCCCCCCCCCCCCCCCCCCCCCCCCCCCCCCCCCCCCCCCCCCCCCCCCCCCCCCCCCC
1220-C
1230- 2 IF (YESTDY.EQ.YRMODE) THEN
1240-C
1250-CCCCCCCCCCCCCCCCCCCCCCCCCCCCCCCCCCCCCCCCCCCCCCCCCCCCCCCCCCCC
1260-C DISTINGUISH BETWEEN DOUBLE AND SINGLE SIZE HISTOGRAMS. C
1270-C READ APPROPRIATE NUMBER OF DATA CARDS. C
1280-CCCCCCCCCCCCCCCCCCCCCCCCCCCCCCCCCCCCCCCCCCCCCCCCCCCCCCCCCCCC
1290-C

```

```

1300-      IF (FLAG.EQ.2) THEN
1310-          LPCNTR=64
1320-          READ(*,30) (DATA(I),I=1,7)
1330-          READ(*,32) (DATA(I),I=8,17)
1340-          READ(*,32) (DATA(I),I=18,27)
1350-          READ(*,30) (DATA(I),I=28,34)
1360-          READ(*,32) (DATA(I),I=35,44)
1370-          READ(*,32) (DATA(I),I=45,54)
1380-          READ(*,32) (DATA(I),I=55,64)
1390-      30  FORMAT(18X,7I6)
1400-      32  FORMAT(10I6)
1410-      ELSE
1420-          LPCNTR=27
1430-          READ(*,30) (DATA(I),I=1,7)
1440-          READ(*,32) (DATA(I),I=8,17)
1450-          READ(*,32) (DATA(I),I=18,27)
1460-      END IF
1470-      C
1480-      CCCCCCCCCCCCCCCCCCCCCCCCCCCCCCCCCCCCCCCCCCCCCCCCCCCCCCCCCCCCC
1490-      C CHECK WAVELENGTH OFFSET. IF IT EQUALS ZERO DETERMINE THE C
1500-      C QUIET SUN BIN LEVEL (QBIN) AND ADD THE AREAS OF ALL BINS C
1510-      C ABOVE THIS VALUE (QBIN+2 TO THE NUMBER OF BINS READ-EITHER C
1520-      C 27 OR 64). PLAGE GENERALLY BEGINS TWO BINS ABOVE QBIN. C
1530-      CCCCCCCCCCCCCCCCCCCCCCCCCCCCCCCCCCCCCCCCCCCCCCCCCCCCCCCCCCCCC
1540-      C
1550-      IF (WAVOFF.EQ.0) THEN
1560-          QBIN=NINT(REAL(QSUN)/1000.0)
1570-          QBIN=QBIN+2
1580-      C
1590-      CCCCCCCCCCCCCCCCCCCCCCCCCCCCCCCCCCCCCCCCCCCCCCCCCCCCCCCCCCCCC
1600-      C SUM THE AREA OF ALL BINS ABOVE THE QUIET SUN LEVEL. C
1610-      CCCCCCCCCCCCCCCCCCCCCCCCCCCCCCCCCCCCCCCCCCCCCCCCCCCCCCCCCCCCC
1620-      C
1630-          DO 60 J=QBIN,LPCNTR
1640-              AREA=DATA(J)+AREA
1650-          60  CONTINUE
1660-      C
1670-      CCCCCCCCCCCCCCCCCCCCCCCCCCCCCCCCCCCCCCCCCCCCCCCCCCCCCCCCCCCCC
1680-      C REJECT THE ENTIRE HISTOGRAM SINCE WAVELENGTH OFFSET IS C
1690-      C OTHER THAN ZERO. C
1700-      CCCCCCCCCCCCCCCCCCCCCCCCCCCCCCCCCCCCCCCCCCCCCCCCCCCCCCCCCCCCC
1710-      C
1720-          ELSE
1730-          GO TO 1
1740-          END IF
1750-      C
1760-      CCCCCCCCCCCCCCCCCCCCCCCCCCCCCCCCCCCCCCCCCCCCCCCCCCCCCCCCCCCCC
1770-      C INITIALIZE AND INCREMENT COUNTER FOR DATA STORAGE ARRAY. C
1780-      CCCCCCCCCCCCCCCCCCCCCCCCCCCCCCCCCCCCCCCCCCCCCCCCCCCCCCCCCCCCC
1790-      C
1800-          I=0
1810-      100  I=I+1
1820-      C

```

```

1830-CCCCCCCCCCCCCCCCCCCCCCCCCCCCCCCCCCCCCCCCCCCCCCCCCCCCCCCCCCCC
1840-C FOR EACH REGION OF A GIVEN DAY, ASSIGN THE FOLLOWING VALUES C
1850-C TO EACH COLUMN: C
1860-C COL 0=USAF REGION NUMBER C
1870-C COL 1=LATITUDE OF REGION VIEWED, C
1880-C COL 2=LONGITUDE OF REGION VIEWED, C
1890-C COL 3=TOTAL AREA OF BRIGHT REGIONS ABOVE QUIET SUN LEVEL C
1900-C (QBIN) IN MILLIONTHS OF THE SOLAR DISK, C
1910-C COL 4=COUNTER FOR NUMBER OF TIMES EACH REGION IS SUPPLE- C
1920-C MENTED BY ANOTHER HISTOGRAM, C
1930-C COL 5=AVERAGE AREA FOR EACH USAF REGION OBSERVED, C
1940-C COL 9=PERCENT OF SOLAR RADIUS (FROM E-W CENTRAL MERIDIAN) C
1950-C WHERE ACTIVE REGION LIES. C
1960-C NOREG=COUNTER FOR NUMBER OF DIFFERENT REGIONS READ PER DAY. C
1970-CCCCCCCCCCCCCCCCCCCCCCCCCCCCCCCCCCCCCCCCCCCCCCCCCCCCCCCCCCCC
1980-C
1990- IF (STORE(I,3).EQ.0.0) THEN
2000- REGONS(I)=REGION
2010- STORE(I,1)=LAT
2020- STORE(I,2)=LON
2030- STORE(I,3)=REAL(AREA)*CAL
2040- STORE(I,4)=1
2050- FOUND=1
2060- NOREG=NOREG+1
2070- ELSE
2080-C
2090-CCCCCCCCCCCCCCCCCCCCCCCCCCCCCCCCCCCCCCCCCCCCCCCCCCCCCCCCCCCC
2100-C A CHECK FOLLOWS TO DETERMINE IF THE LATEST REGION IS C
2110-C ONE PREVIOUSLY MEASURED OR A NEW ONE. IF IT IS A NEW C
2120-C REGION, ANOTHER ROW IS STARTED IN THE STORAGE ARRAY. C
2130-CCCCCCCCCCCCCCCCCCCCCCCCCCCCCCCCCCCCCCCCCCCCCCCCCCCCCCCCCCCC
2140-C
2150- IF (REGION.EQ.REGONS(I)) THEN
2160-C
2170-CCCCCCCCCCCCCCCCCCCCCCCCCCCCCCCCCCCCCCCCCCCCCCCCCCCCCCCCCCCC
2180-C IF THE CURRENT REGION DOES NOT DIFFER FROM ONE PREVIOUSLY C
2190-C MEASURED, THEN ADD THE CURRENT REGION TO THE TOTAL AREA FOR C
2200-C THAT REGION. FOUND IS A FLAG INDICATING WHETHER OR NOT AN C
2210-C EXISTING REGION WAS SUPPLEMENTED OR A NEW ONE WAS ENCOUN- C
2220-C TERED. FOUND=1 MEANS DATA HAS BEEN STORED IN THE ARRAY AND C
2230-C ANOTHER HISTOGRAM MUST BE READ. FOUND=0 INDICATES DATA HAS C
2240-C NOT BEEN STORED AND THE NEXT REGION MUST BE COMPARED. C
2250-CCCCCCCCCCCCCCCCCCCCCCCCCCCCCCCCCCCCCCCCCCCCCCCCCCCCCCCCCCCC
2260-C
2270- STORE(I,3)=STORE(I,3)+REAL(AREA)*CAL
2280- STORE(I,4)=STORE(I,4)+1.0
2290- FOUND=1
2300- END IF
2310- IF (FOUND.NE.1) THEN
2320- GO TO 100
2330- END IF
2340- END IF
2350-C
2360- FOUND=0
2370- AREA=0
2380- GO TO 1
2390-C
2400-CCCCCCCCCCCCCCCCCCCCCCCCCCCCCCCCCCCCCCCCCCCCCCCCCCCCCCCCCCCC
2410-C WHEN THE NEXT CARD IN THE SEQUENCE SPECIFIES A NEW DAY, THE C
2420-C PREVIOUS DAY'S INFORMATION MUST BE SUMMARIZED. C
2430-CCCCCCCCCCCCCCCCCCCCCCCCCCCCCCCCCCCCCCCCCCCCCCCCCCCCCCCCCCCC
2440-C

```

```

2450-      ELSE
2460-C
2470-C CCCCCCCCCCCCCCCCCCCCCCCCCCCCCCCCCCCCCCCCCCCCCCCCCCCCCCCCCCCCC
2480-C FOR EACH REGION OBSERVED IN A DAY, DETERMINE THE AVERAGE C
2490-C AREA (-TOTAL AREA/NUMBER OF OBSERVATIONS). C
2500-C CCCCCCCCCCCCCCCCCCCCCCCCCCCCCCCCCCCCCCCCCCCCCCCCCCCCCCCCCCCCC
2510-C
2520-      DO 200 I=1,NOREG
2530-      STORE(I,5)=STORE(I,3)/STORE(I,4)
2540- 200 CONTINUE
2550-C
2560-C CCCCCCCCCCCCCCCCCCCCCCCCCCCCCCCCCCCCCCCCCCCCCCCCCCCCCCCCCCCCC
2570-C SEARCH THROUGH THE ALFA MATRIX UNTIL THE DATE OF THE DAY'S C
2580-C DATA BEING SUMMARIZED MATCHES THE DATE OF THE APPROPRIATE C
2590-C P, BO, AND LO. USE THESE VALUES FOR SUMMARY CALCULATIONS. C
2600-C CCCCCCCCCCCCCCCCCCCCCCCCCCCCCCCCCCCCCCCCCCCCCCCCCCCCCCCCCCCCC
2610-C
2620-      DO 205 N=1,EPHDAY
2630-      DAY=INT(ALFA(N,1))
2640-      IF (DAY.EQ.YESTDY) THEN
2650-      P=ALFA(N,2)*(RAD/360)
2660-      BO=ALFA(N,3)*(RAD/360)
2670-      END IF
2680- 205 CONTINUE
2690-C
2700-C CCCCCCCCCCCCCCCCCCCCCCCCCCCCCCCCCCCCCCCCCCCCCCCCCCCCCCCCCCCCC
2710-C FOR EACH REGION ENCOUNTERED, ACCOUNT FOR FORESHORTENING C
2720-C USING THE SECANT RULE. CALCULATE THE CORRECTED AREA (COL 7, C
2730-C STORE(I,6)) AS IF THE SUN WERE BEING VIEWED DIRECTLY ABOVE C
2740-C THAT POINT. THETA IS THE ANGLE BETWEEN THE CENTER POINT OF C
2750-C THE SUN AND THE CENTER POINT OF THE OBSERVED REGION. C
2760-C IT GIVES AN INDICATION OF HOW FAR FROM THE CENTERLINE OF C
2770-C THE SUN THE VIEWED REGION IS. THE SECANT CORRECTION IS C
2780-C INACCURATE FOR LONGITUDES GREATER THAN 65 DEGREES. C
2790-C DATA FOR LONGITUDES GREATER THAN 90 DEGREES MUST BE C
2800-C DISCARDED. C
2810-C CCCCCCCCCCCCCCCCCCCCCCCCCCCCCCCCCCCCCCCCCCCCCCCCCCCCCCCCCCCCC
2820-C
2830-      DO 210 I=1,NOREG
2840-      A=ABS(STORE(I,2))
2850-      B=(RAD/4)-STORE(I,1)
2860-      C=(RAD/4)-BO
2870-      THETA=ACOS(COS(B)*COS(C)+SIN(B)*SIN(C)*COS(A))
2880-      STORE(I,6)=STORE(I,5)*(1.0/COS(THETA))
2890-C
2900-C CCCCCCCCCCCCCCCCCCCCCCCCCCCCCCCCCCCCCCCCCCCCCCCCCCCCCCCCCCCCC
2910-C ACCOUNT FOR SOLAR INCLINATION TO THE ECLIPTIC AND ITS VAR- C
2920-C IATION DUE TO THE EARTH'S ROTATION ABOUT THE SUN. THIS C
2930-C COORDINATE TRANSFORMATION GIVES THE LATITUDE AND LONGITUDE C
2940-C OF ACTIVE REGIONS AS VIEWED FROM EARTH IN THE REFERENCE C
2950-C FRAME OF THE ALGONQUIN DATA (LAT-COL 8, LONG-COL 9). C
2960-C CCCCCCCCCCCCCCCCCCCCCCCCCCCCCCCCCCCCCCCCCCCCCCCCCCCCCCCCCCCCC
2970-C

```

```

2980-      LOS=COS(BO)*COS(STORE(I,1))*COS(STORE(I,2))
2990-      +      -SIN(BO)*SIN(STORE(I,1))
3000-      STORE(I,9)=SIN(P)*SIN(BO)*COS(STORE(I,1))*COS(STORE(I,2))
3010-      +      +COS(P)*COS(STORE(I,1))*SIN(STORE(I,2))
3020-      +      +SIN(P)*COS(BO)*SIN(STORE(I,1))
3030-      Z=SIN(BO)*COS(P)*COS(STORE(I,1))*COS(STORE(I,2))
3040-      +      -SIN(P)*COS(STORE(I,1))*SIN(STORE(I,2))
3050-      +      +COS(P)*COS(BO)*SIN(STORE(I,1))
3060-      STORE(I,7)=PI/2-ACOS(Z/SQRT(LOS**2+STORE(I,9)**2+Z**2))
3070-      STORE(I,8)=ATAN(STORE(I,9)/LOS)
3080- 210  CONTINUE
3090-C
3100-CCCCCCCCCCCCCCCCCCCCCCCCCCCCCCCCCCCCCCCCCCCCCCCCCCCCCCCCCCCC
3110-C PRINT OUT DAILY SUMMARY TABLE.  LATITUDE AND LONGITUDE IN  C
3120-C DEGREES.  AREA IN MILLIONTHS OF THE SOLAR DISK.  C
3130-CCCCCCCCCCCCCCCCCCCCCCCCCCCCCCCCCCCCCCCCCCCCCCCCCCCCCCCCCCCC
3140-C
3150-      PRINT*, ' '
3160-      PRINT(' SUMMARY TABLE FOR DATE:',I7,', IS:'),YESTDY
3170-      WRITE(*,250)
3180- 250  FORMAT(2X,'REGION',2X,'LAT',4X,'LONG',4X,'TOTAL AREA',
3190-      +      2X,'OBSV',2X,'AVG AREA',3X,'COR AREA',3X,'NLAT',
3200-      +      4X,'NLONG',3X,'SOLRAD')
3210-C
3220-      DO 260 I=1,NOREG
3230-          STORE(I,1)=STORE(I,1)*(360/RAD)
3240-          STORE(I,2)=STORE(I,2)*(360/RAD)
3250-          STORE(I,7)=STORE(I,7)*(360/RAD)
3260-          STORE(I,8)=STORE(I,8)*(360/RAD)
3270- 260  CONTINUE
3280-C
3290-      DO 230 I=1,NOREG
3300-          WRITE(*,(' ',1X,A4,2X,F7.2,1X,F7.2,1X,F11.2,2X,F3.0,
3310-      +      2X,F10.2,1X,F10.2,1X,F7.2,1X,F7.2,3X,F4.2))
3320-      +      (REGONS(I)),(STORE(I,J),J=1,9)
3330- 230  CONTINUE
3340-C
3350-CCCCCCCCCCCCCCCCCCCCCCCCCCCCCCCCCCCCCCCCCCCCCCCCCCCCCCCCCCCC
3360-C INITIALIZE STORAGE ARRAY AND VARIABLES IN PREPARATION FOR  C
3370-C ANOTHER DAY'S DATA.  C
3380-CCCCCCCCCCCCCCCCCCCCCCCCCCCCCCCCCCCCCCCCCCCCCCCCCCCCCCCCCCCC
3390-C
3400-      DO 270 I=1,NOREG
3410-          DO 280 J=1,9
3420-              STORE(I,J)=0.0
3430- 280  CONTINUE
3440- 270  CONTINUE
3450-C
3460-      DO 275 I=1,14
3470-          REGONS(I)= ' '
3480- 275  CONTINUE
3490-C
3500-      NOREG=0
3510-      P=0.0
3520-      BO=0.0
3530-      A=0.0
3540-      B=0.0
3550-      C=0.0
3560-      Z=0.0
3570-      LOS=0.0
3580-      THETA=0.0
3590-      YESTDY=YRMODA
3600-C

```

```
3610-CCCCCCCCCCCCCCCCCCCCCCCCCCCCCCCCCCCCCCCCCCCCCCCCCCCCCCCCCCCC
3620-C SINCE THE FIRST CARD OF A NEW DAY CAUSED THE SUMMARY REPORT C
3630-C TO BE CALCULATED, RETURN AND START WITH THE DATA FOR THIS C
3640-C HISTOGRAM ON A NEW DAY. C
3650-CCCCCCCCCCCCCCCCCCCCCCCCCCCCCCCCCCCCCCCCCCCCCCCCCCCCCCCCCCCC
3660-C
3670- GO TO 2
3680- END IF
3690- 300 STOP
3700- END
3710-*EOR
```

APPENDIX E

Coordinate Transformation

This coordinate transformation algorithm was used in the SOON Program to transpose the latitude and longitude from the SOON coordinate frame to the Algonquin frame to aid in direct comparison of the data. X, Y, Z is the heliocentric frame. The east-west frame is x, y, z.

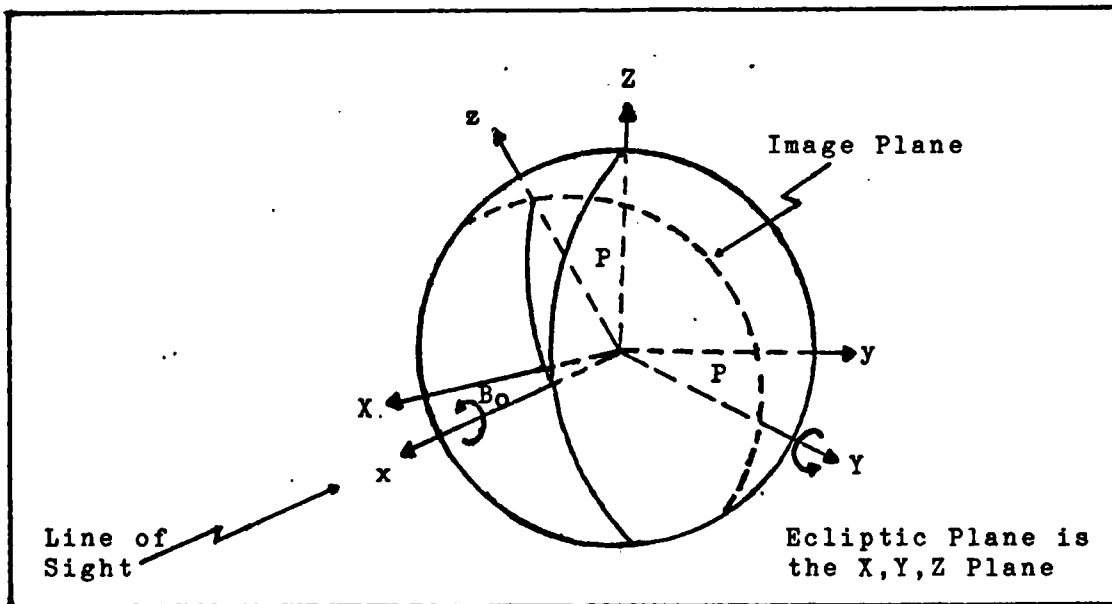


Figure 11. Frame Orientations

Rotations

The first transformation is a positive or negative rotation about Y by an angle B_0 .

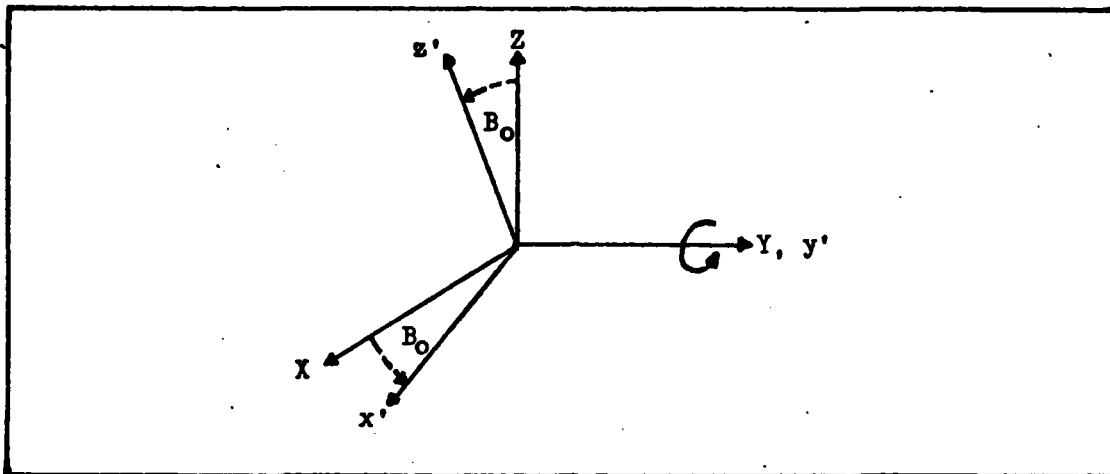


Figure 12. Rotation about Y

The second transformation is a positive or negative rotation about x by an angle P (Ref 25:8-13).

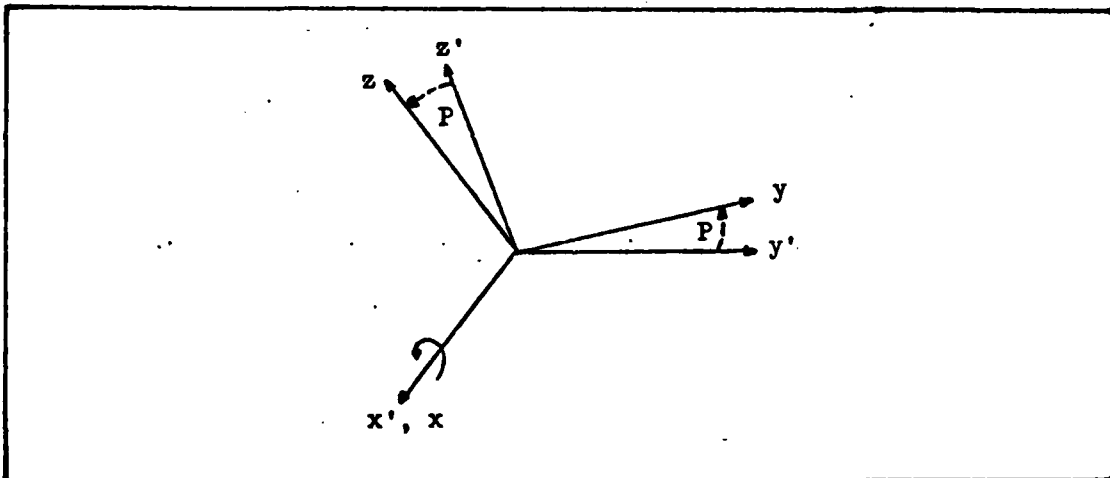


Figure 13. Rotation about x

Orthogonal Transformations

For two positive rotations:

$$\begin{bmatrix} x' \\ y' \\ z' \end{bmatrix} = \begin{bmatrix} \cos B_0 & 0 & -\sin B_0 \\ 0 & 1 & 0 \\ \sin B_0 & 0 & \cos B_0 \end{bmatrix} \begin{bmatrix} X \\ Y \\ Z \end{bmatrix} = \gamma \begin{bmatrix} X \\ Y \\ Z \end{bmatrix} \quad (25)$$

$$\begin{bmatrix} x \\ y \\ z \end{bmatrix} = \begin{bmatrix} 1 & 0 & 0 \\ 0 & \cos P & \sin P \\ 0 & -\sin P & \cos P \end{bmatrix} \begin{bmatrix} x' \\ y' \\ z' \end{bmatrix} = \beta \begin{bmatrix} x' \\ y' \\ z' \end{bmatrix} \quad (26)$$

therefore,

$$\begin{bmatrix} x \\ y \\ z \end{bmatrix} = \beta \gamma \begin{bmatrix} X \\ Y \\ Z \end{bmatrix} = \alpha \begin{bmatrix} X \\ Y \\ Z \end{bmatrix} \quad (27)$$

where

$$\alpha = \begin{bmatrix} \cos B_0 & 0 & -\sin B_0 \\ \sin P \sin B_0 & \cos P & \sin P \cos B_0 \\ \sin B_0 \cos P & -\sin P & \cos P \cos B_0 \end{bmatrix} \quad (28)$$

To obtain X, Y, and Z a spherical to rectangular coordinate transformation must be done (Ref 34:36)

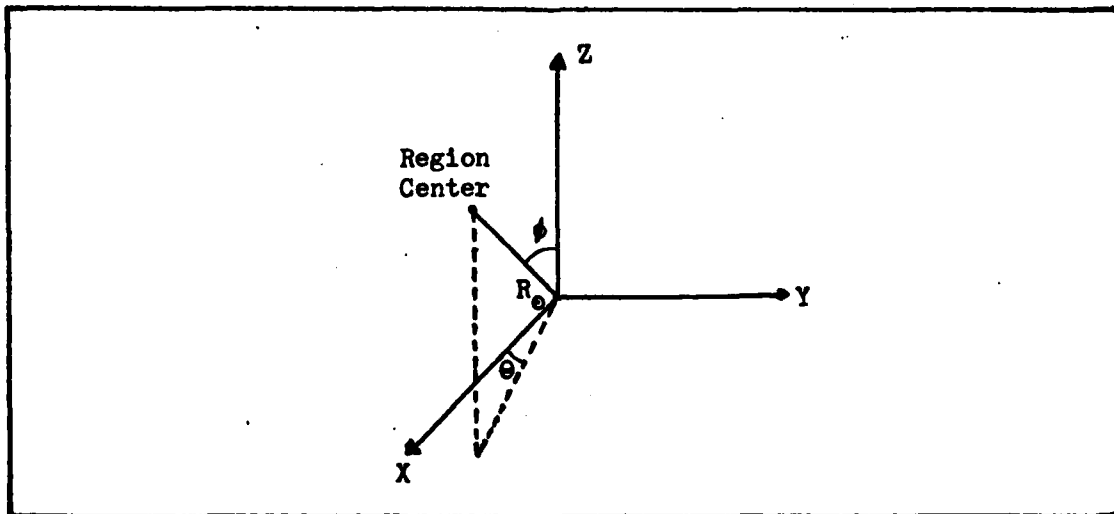


Figure 14. Spherical to Rectangular Coordinate Transformation

such that

$$\begin{aligned} X &= R_{\odot} \sin \phi \cos \theta \\ &= R_{\odot} \cos (L_r) \cos (A_r) \end{aligned} \quad (29)$$

where

$$\begin{aligned} R_{\odot} &= \text{radius of the sun,} \\ L_r &= \text{heliocentric latitude of the region on the sun, and} \\ A_r &= \text{central meridian angle (heliocentric) .} \end{aligned}$$

Similarly,

$$Y = R_{\odot} \cos (L_r) \sin (A_r) \quad (30)$$

and

$$Z = R_{\odot} \sin (L_r) \quad (31)$$

Therefore,

$$x = \cos B_0 R_{\odot} \cos (L_r) \cos (A_r) - \sin B_0 R_{\odot} \sin (L_r) , \quad (32)$$

$$\begin{aligned} y &= \sin P \sin B_0 R_{\odot} \cos (L_r) \cos (A_r) \\ &\quad + \cos P R_{\odot} \cos (L_r) \sin (A_r) \\ &\quad + \sin P \cos B_0 R_{\odot} \sin (L_r) , \end{aligned} \quad (33)$$

and

$$\begin{aligned} z &= \sin B_0 \cos P R_{\odot} \cos (L_r) \cos (A_r) \\ &\quad - \sin P R_{\odot} \cos (L_r) \sin (A_r) \\ &\quad + \cos P \cos B_0 R_{\odot} \sin (L_r) \end{aligned} \quad (34)$$

The data was unitized to solar radii by setting $R_{\odot}=1.0$.

To go back to latitude and central meridian angle in the east-west frame, a rectangular to spherical transformation is performed:

$$\tan \lambda_r = y / x \quad (35)$$

then

$$\lambda_r = \tan^{-1}(y / x), \quad x \neq 0 \quad (36)$$

and

$$\cos (90 - \lambda_r) = z / \sqrt{x^2 + y^2 + z^2} \quad (37)$$

therefore

$$\lambda_r = 90 - \cos^{-1} [z / \sqrt{x^2 + y^2 + z^2}] \quad (38)$$

where

λ_r = east-west frame central meridian angle (longitude)

and

λ_r = east-west frame latitude.

In the SOON Program

x = LOS (line of site), and

y = STORE (I,9).

APPENDIX F

Data Analysis Programs

The following programs, ANAL1 and ANAL3, were used to analyze the data for this project. ANAL1 provides a scatter-gram of the data while ANAL3 gives a more complete breakdown of the results of the analysis including the residuals used to determine the adequacy of the model. These basic programs, with minor modifications, were used to test the data after removing some of the data points. ANAL3 was used to find more significant digits for the predictive equations by multiplying each NEWSCH and NEWAREA value by 1000 on one run.

100-CAP,CM60000,T100,IO120. T820740,PUZ,4172
110-ATTACH,SPSS,ID-AFIT.
120-SPSS.
130-#EOR
140-RUN NAME CALSCN VS SOONAREA NOV82 ANAL1
150-VARIABLE LIST DATE,CALSCN,SOONAREA
160-VAR LABELS CALSCN CALIBRATED OTTAWA SCAN VALUES/
170- SOONAREA CORRECTED AREA FROM SOON HISTOGRAMS
180-INPUT FORMAT FREEFIELD
190-N OF CASES 142
200-COMPUTE NEWSCN=CALSCN/SOONAREA
210-COMPUTE NEWAREA=1/SOONAREA
220-PRINT FORMAT CALSCN (2),SOONAREA (2),NEWSCN (6),NEWAREA (6)
230-LIST CASES CASES=142/VARIABLES=DATE,CALSCN,SOONAREA,
240- NEWSCN,NEWAREA
250-SCATTERGRAM NEWSCN WITH NEWAREA
260-STATISTICS ALL
270-READ INPUT DATA
280-780501 4.82 13686.81
290-780504 4.70 26714.89
300-...
310-FINISH

100-CAP,CM60000,T100,IO120. T820740,PUZ,4172
 110-ATTACH,SPSS,ID=AFIT.
 120-SPSS.
 130-*EOR
 140-RUN NAME CALSCN VS SOONAREA NOV82 ANAL3
 150-VARIABLE LIST DATE,CALSCN,SOONAREA
 160-VAR LABELS CALSCN CALIBRATED OTTAWA SCAN VALUES/
 170- SOONAREA CORRECTED AREA FROM SOON HISTOGRAMS
 180-INPUT FORMAT FREEFIELD
 190-N OF CASES 142
 200-COMPUTE NEWSCN=CALSCN/SOONAREA
 210-COMPUTE NEWAREA=1/SOONAREA
 220-PRINT FORMAT CALSCN (2),SOONAREA (2),NEWSCN (6),NEWAREA (6)
 230-LIST CASES CASES=142/VARIABLES=DATE,CALSCN,SOONAREA,
 240- NEWSCN,NEWAREA
 250-REGRESSION METHOD=FORWARD/
 260- VARIABLES=NEWSCN,NEWAREA/
 270- REGRESSION=NEWSCN WITH NEWAREA/
 280- RESIDUALS/
 290-STATISTICS ALL
 300-READ INPUT DATA
 310-780501 4.82 13686.81
 320-780504 4.70 26714.89
 330-...
 340-FINISH

VITA

Craig Anton Puz was born on 24 June 1954 in Pasadena, California. He graduated from Edgewood High School in West Covina, California, in 1972 and attended the United States Air Force Academy, Colorado Springs, Colorado, from which he received the degree of Bachelor of Science in General Studies in June 1976. Upon graduation he reported to the 90th Strategic Missile Wing at F. E. Warren Air Force Base, Cheyenne, Wyoming, where he served as a Minuteman III Missile Combat Crewmember, Training Division instructor, and Emergency War Order instructor. While at F. E. Warren, he also earned a Master of Business Administration degree through the Air Force Institute of Technology sponsored, University of Wyoming masters program. He served at F. E. Warren until entering the School of Engineering Space Operations masters program, Air Force Institute of Technology, in 1981.

Permanent Address: 1916 Kenoak Drive
West Covina, California 91790

UNCLASSIFIED

SECURITY CLASSIFICATION OF THIS PAGE (When Data Entered)

REPORT DOCUMENTATION PAGE		READ INSTRUCTIONS BEFORE COMPLETING FORM										
1. REPORT NUMBER AFIT/GSO/MA/82D-2	2. GOVT ACCESSION NO. AD A124892	3. RECIPIENT'S CATALOG NUMBER										
4. TITLE (and Subtitle) CORRELATING RADIO EMISSIONS WITH VISIBLE EMISSIONS FROM INDIVIDUAL SOLAR ACTIVE REGIONS		5. TYPE OF REPORT & PERIOD COVERED MS Thesis										
		6. PERFORMING ORG. REPORT NUMBER										
7. AUTHOR(s) Craig A. Puz Capt		8. CONTRACT OR GRANT NUMBER(s)										
9. PERFORMING ORGANIZATION NAME AND ADDRESS Air Force Institute of Technology (AFIT-EN) Wright-Patterson AFB, Ohio 45433		10. PROGRAM ELEMENT, PROJECT, TASK AREA & WORK UNIT NUMBERS										
11. CONTROLLING OFFICE NAME AND ADDRESS Air Force Global Weather Central Offutt Air Force Base, Nebraska 68513		12. REPORT DATE December 1982										
		13. NUMBER OF PAGES 77										
14. MONITORING AGENCY NAME & ADDRESS (if different from Controlling Office)		15. SECURITY CLASS. (of this report) Unclassified										
		15a. DECLASSIFICATION/DOWNGRADING SCHEDULE										
16. DISTRIBUTION STATEMENT (of this Report) Approved for public release; distribution unlimited												
17. DISTRIBUTION STATEMENT (of the abstract entered in Block 20, if different from Report)		2861 JAN 1982 4										
18. SUPPLEMENTARY NOTES		Approved for public release; IAW AFR 190-17. LYNN E. WOLAVER Dean for Research and Professional Development Air Force Institute of Technology (ATC) Wright-Patterson AFB OH 45433										
Approved for public release; IAW AFR 190-17 Frederick C. Lynch, Major, USAF Director of Information												
19. KEY WORDS (Continue on reverse side if necessary and identify by block number)												
<table border="0"> <tr> <td>SOON</td> <td>Solar Activity</td> </tr> <tr> <td>Solar Observing Optical Network</td> <td>Solar Phenomena Predictive Models</td> </tr> <tr> <td>Solar Radio Flux</td> <td>10.7 CM Solar Radio Flux</td> </tr> <tr> <td>Solar Radio Emissions</td> <td>Statistical Regression</td> </tr> <tr> <td>Solar Visible Emissions</td> <td></td> </tr> </table>			SOON	Solar Activity	Solar Observing Optical Network	Solar Phenomena Predictive Models	Solar Radio Flux	10.7 CM Solar Radio Flux	Solar Radio Emissions	Statistical Regression	Solar Visible Emissions	
SOON	Solar Activity											
Solar Observing Optical Network	Solar Phenomena Predictive Models											
Solar Radio Flux	10.7 CM Solar Radio Flux											
Solar Radio Emissions	Statistical Regression											
Solar Visible Emissions												
20. ABSTRACT (Continue on reverse side if necessary and identify by block number)												
<p>Using a statistical regression model, a relationship was found between the area of solar active regions (bright in hydrogen-alpha, $\lambda = 6562.8 \text{ \AA}$ in the visible) and their 10.7 cm radio emission. Data used in this analysis were the brightness-area histograms obtained from the Solar Observing Optical Network (SOON) and daily drift scans obtained from the Algonquin Radio Observatory, Ottawa, Canada. This data, for the period 1 May through 16 July 1978, was used to develop the following relationship:</p> <p>Algonquin Scan Peak Value = $.88782838 + .00025237604$ (Calibrated SOON Area)</p>												

D
33